MAGNETIC STORM CHARACTERISTICS
OF THE THERMOSPHERE

H. G. MAYR

H. VOLLAND

SEPTEMBER 1972

GSFC —— GODDARD SPACE FLIGHT CENTER ——
GREENBELT, MARYLAND

MAGNETIC STORM CHARACTERISTICS

OF THE THERMOSPHERE

by

H. G. Mayr

Goddard Space Flight Center

and

H. Volland

University of Bonn

ABSTRACT

Energy and diffusive mass transport associated with the thermospheric

circulation are considered in a self-consistent, though mathematically relatively

simple form to describe in a three-dimensional two-constituent model magnetic

storm characteristics in composition (N_2, O, and He), temperature and mass-

density. It is shown that during disturbed conditions the latitudinal variations

of composition and gas temperature T_g reflect the local nature of the magnetic

storm heat input assumed to be primarily confined to the auroral zones. There-

by T_g and N_2 increase, He decreases and O remains constant through the

auroral zones at exospheric heights (due to the superposition of temperature and

diffusion effects) in agreement with OGO-6 mass spectrometer measurements.

In contrast, the magnetic storm response in the total mass density is character-

ized by a strong world-wide component and a relatively insignificant increase

toward the poles with the density peak occurring between two (poles) and eight

(equator) hours after the maximum energy input, in substantial agreement with

satellite drag data. While in situ composition and satellite drag mass-density

measurements can thus be reconciled it must, however, be emphasized that the

temperature derivation from the satellite drag data cannot be justified during

disturbed conditions.

I. INTRODUCTION

Jacchia (1959) and Jacchia et al., (1967) have shown that the thermospheric density increases during geomagnetic disturbances with the effect being proportional to the planetary index A_p for large disturbances and to the index K_p for small disturbances. Furthermore it has been observed from satellite drag data that the effect occurs worldwide but is systematically stronger at higher latitudes (Roemer, 1967).

In a recent paper by Taeusch et al. (1971) OGO 6 mass spectrometer data were presented which revealed at 400 km:

(a) a gradual increase in N_2 toward high latitudes (up to a factor of 10 for $A_p = 130$),

(b) an increase in the exospheric temperature (from 1000 to 1400°K) at high latitudes which was inferred from the variation in N_2, and

(c) negligible latitude variations in O.

Volland and Mayr (1971) treated the magnetic storm response of the thermosphere in a simple analytical model. Assuming that the energy source is confined to auroral zones at ±65° we expanded this input into a series of spherical harmonics (P_n)

$$Q = \Sigma \, q_n \, P_n = Q_0 \, (P_0 + 3.66 \, P_2 + 2.22 \, P_4 - 2.65 \, P_6 \cdots)$$

which, as expected, converges slowly. However, due to the importance of advective energy exchange, associated with the thermospheric circulation, the efficiency for the excitation of density variations decreases with the power of about $1/n^2$ and consequently higher order terms produce only small contributions for the density structure. This characteristic thus explained the observed worldwide component as well as the gradual increase toward higher latitudes in the thermospheric mass density during magnetic storms.

It was shown by Mayr and Volland (1970, 1972a) that during disturbed conditions the thermospheric circulation effectively redistributes the minor constituents such as to reduce the oxygen concentration at high latitudes and within the lower thermosphere. Since this depletion is associated with a thermal expansion both effects tend to cancel each other in the upper thermosphere hence explaining the negligible response in O at times when the N_2 concentration is observed to increase (Taeusch et al., 1971). In that paper we restricted ourselves to a very simple model by postulating that in a first approximation

(a)   the latitude dependence in the form of P_2 (θ) dominates,

(b)   a diffusion model can be adopted in which the momentum feedback from the minor to the major constituent is negligible, and

(c)   the effect of the diffusive redistribution can be neglected for the energetics.

Although none of these simplifying assumptions affected our earlier conclusions substantially, it will be shown in this paper that by relaxing them a number

of important features evolve which further characterize the magnetic storm response in the thermosphere.

II. QUALITATIVE DISCUSSION

Figure 1 shows a simplified block diagram for the thermosphere dynamics. It illustrates the links between the composition and gas temperature on one hand and the various physical processes and atmospheric parameters on the other hand.

Suppose the heat input Q is known as a function of time and space defined with height and latitude. Some of the energy is conducted down into the lower atmosphere thus affecting the temperature distribution and with that the composition.

However, a second and not less important energy drain goes through the global circulation which is significantly affected by ion collisions. In this mechanism which is explicitly neglected in one dimensional models energy is exchanged through advection and this in turn affects the temperature and the thermospheric composition.

In parallel the thermospheric circulation induces diffusion which depends to various degrees upon the eddy diffusion coefficient, and this diffusion process affects the composition directly. Any variations in the composition are associated with variations in the partial and total pressure fields. This in turn influences the global circulation and with that advection and with that again temperature and composition. So it is apparent that all the processes

surrounded by the dashed box in Figure 1 are interconnected. In fact it has been shown that the links between diffusion and energetics are extremely important in the seasonal variations of the thermosphere where the diffusion process can account for an increase in the temperature amplitude by as much as a factor of three (Mayr and Volland, 1972b).

The efficiency for the excitation of variations in the thermosphere depends on a number of properties such as those emphasized in Figure 2. These are related to

(a) heat conductivity

(b) ion collision frequency and viscosity

(c) eddy and molecular diffusion coefficients and

(d) horizontal, vertical and time scales of Q.

The significance of these properties becomes apparent when looking at simple algebraic equations which describe the continuity of momentum, mass and energy.

Attributing characteristic lengths to the energy input's time duration (τ) and horizontal (ℓ) and vertical (h) scales, and replacing all differential operators by

$$\frac{\partial}{\partial t} \propto \frac{1}{\tau}, \qquad \frac{1}{r} \frac{\partial}{\partial \theta} \propto \frac{1}{\ell}, \qquad \frac{\partial}{\partial r} \propto \frac{1}{h} \qquad (1)$$

where

$$t = time$$

$$\theta = latitude$$

$$z = height,$$

the continuity equations take the simplified forms

$$\Delta \rho \propto \Delta p \propto c \, \Delta T \tag{2}$$

for the vertical momentum equation,

$$U \propto \frac{\dfrac{p}{\rho}}{\ell \left(\nu + \dfrac{\epsilon}{\rho h^2} \right)} \Delta \rho \tag{3}$$

for the horizontal momentum equation

$$W \propto \frac{\left[\dfrac{\dfrac{p}{\rho}}{\ell^2 \left(\nu + \dfrac{\epsilon}{\rho h^2} \right)} + \dfrac{i}{\tau} \right]}{\left(\dfrac{1}{H} - \dfrac{1}{h} \right)} \Delta \rho \tag{4}$$

for the continuity equation and

$$\Delta \rho \propto \frac{\dfrac{Q}{p}}{\dfrac{mK}{h^2 k \rho c} + \dfrac{\dfrac{p}{\rho}}{\ell^2 H \left(\dfrac{1}{H} - \dfrac{1}{h} \right) \left(\nu + \dfrac{\epsilon}{\rho h^2} \right)} + \dfrac{i}{\tau} \left(\dfrac{1}{h \left(\dfrac{1}{H} - \dfrac{1}{h} \right)} + \dfrac{3}{2c} \right)} \tag{5}$$

for the energy equation.

In the equations (2) through (5) all constants and quantities have been omitted except those essential to identify a particular process. So c characterizes

a constant proportional to the mass m of the constituent, ν ion collisions, ϵ viscosity, H scale height, K heat conductivity, k Boltzmann's constant and i indicates a phase difference of 90° due to the time derivative. $\Delta\rho$, ΔT and Δp are the relative variations of mass density, temperature and pressure respectively, p and ρ are the time average pressure and mass density and U and W are the meridional and vertical velocities respectively. Q is the amplitude of the heat input. The effects from the Coriolis force and thus zonal winds are not considered in this discussion. In the denominator of Eq. (5) the first term represents heat conduction, the second one represents advection and the third term represents the energy contributions that go into breathing and internal energy.

For a minor constituent with a relative density amplitude $\Delta\rho_m$ and a vertical scale height H_m the diffusion velocity $W_D = W_m - W$ is derived from the continuity equation

$$W_D \propto \frac{i\,\dfrac{\Delta\rho_m}{\tau} - W\left(\dfrac{1}{H_m} - \dfrac{1}{h_m}\right) + \dfrac{U}{\ell}}{\left(\dfrac{1}{H_m} - \dfrac{1}{h_m}\right)} = \frac{\dfrac{i}{\tau}(\Delta\rho_m - \Delta\rho) + W\left(\dfrac{1}{H} - \dfrac{1}{H_m} - \dfrac{1}{h} + \dfrac{1}{h_m}\right)}{\left(\dfrac{1}{H_m} - \dfrac{1}{h_m}\right)} \qquad (6)$$

where h_m is the scale height of W_m, and its density is

$$\Delta\rho_m \propto c_m \Delta T - \frac{W_D}{D} \qquad (7)$$

where D is a factor proportional to the diffusion coefficient. Combinding Eq. (5) with Eq. (7) yields

$$\Delta \rho_m \underset{\sim}{\propto} \cfrac{c_m \Delta T + \cfrac{\cfrac{i}{\tau D}\Delta \rho - \cfrac{W}{D}\left(\cfrac{1}{H} - \cfrac{1}{H_m} - \cfrac{1}{h} + \cfrac{1}{h_m}\right)}{\left(\cfrac{1}{H_m} - \cfrac{1}{h_m}\right)}}{\left(1 + \cfrac{i}{\tau D\left(\cfrac{1}{H_m} - \cfrac{1}{h_D}\right)}\right)} \tag{8}$$

Thereby c_m is (analogous to Eq. 3) proportional to the mass of the constituent.

Assuming that in   first approximation the diffusion process does not affect the total internal energy or the total pressure variations, we can estimate the diffusion effect upon the temperature. Let ΔT be the temperature variation under the assumption of   diffusive equilibrium and ΔT_D the temperature variation with diffusion; then the relation

$$\Delta T_D \approx \Delta T + \frac{\rho_m}{(c_m \rho + c_m \rho_m)} \frac{W_D}{D} \tag{9}$$

can be derived neglecting for simplicity the temperature components in the pressure variations. ΔT is due to the diffusive equilibrium assumption of course a fictitious quantity while ΔT_D is considered to be a realistic representation of the actual variations in the gas temperature T_g.

Although heat conduction is the primary energy transport mechanism for the spatially uniform component in the thermosphere, it plays a relatively minor role in spatially non uniform components where the thermospheric circulation competes in the redistribution of energy. Thus the second term in the denominator of Eq. 5, describing the advective energy loss, is generally larger than the first one

which describes the heat conduction loss. Defining a characteristic time for the advective energy exchange

$$\tau_c \approx \frac{\ell^2 \left(\nu + \dfrac{\epsilon}{\rho h^2} \right)}{\dfrac{p}{\rho}}$$

Eq. 5 can be further simplified to yield for the latitude dependent component

$$\Delta \rho \approx \ell^2 \ H \left(\frac{1}{H} - \frac{1}{h} \right) \left(\nu + \frac{\epsilon}{\rho h^2} \right) \frac{\rho}{p^2} \ Q \tag{10}$$

for $\tau \gg \tau_c$ and

$$\Delta \rho \approx - \frac{i \ \tau}{\left(\dfrac{1}{h \left(\dfrac{1}{H} - \dfrac{1}{h} \right)} + \dfrac{3}{2 \ c} \right)} \frac{Q}{p} \tag{11}$$

for $\tau \ll \tau_c$.

τ_c is generally of the order of half a day; it depends however upon the electron density as well as on the scale height, h, and the thermospheric density, ρ. Since the time duration of magnetic storms is typically of the order one or two days, relation (10) is approximately applicable. This shows then that the amplitude of the latitude dependent component tends to be proportional to the square of the horizontal scale, ℓ, and to the ion collision frequency ν. The characteristics of the density variations, expressed in (10) and (11) have been discussed in detail by Volland and Mayr (1971).

Substituting Eq. 10 into (3) and (6) the following relations can be deduced for the wind field

$$U \propto \ell \, H \left(\frac{1}{H} - \frac{1}{h} \right) \frac{Q}{p} \tag{12}$$

$$W \propto H \frac{Q}{p} \tag{13}$$

which shows that the vertical wind velocity tends to be independent of the horizontal scale ℓ. Similarly, the diffusion effect for the minor constituents (see Eq. 8), which is proportional to W, is then also independent of the horizontal scale, and the variations of the minor constituents can be expressed in the form

$$\Delta \rho_m \propto c_m \, \Delta T - \frac{\frac{H}{D} \left(\frac{1}{H} - \frac{1}{H_m} - \frac{1}{h} + \frac{1}{h_m} \right)}{\left(\frac{1}{H_m} - \frac{1}{h_m} \right)} \frac{Q}{p} \tag{14}$$

Considering Eqs. (2) and (10) the temperature variation, including diffusion (see Eq. 9), takes the final form

$$\Delta T_D \propto \left\{ \ell^2 \frac{H}{c} \left(\frac{1}{H} - \frac{1}{h} \right) \left(\nu + \frac{\epsilon}{\rho \, h^2} \right) \frac{\rho}{p} + \frac{H}{D} \frac{\rho_m}{(c_m \rho + c_m \rho_m)} \frac{\left(\frac{1}{H} - \frac{1}{H_m} - \frac{1}{h} + \frac{1}{h_m} \right)}{\left(\frac{1}{H_m} - \frac{1}{h_m} \right)} \right\} \frac{Q}{p} \, . \tag{15}$$

The first term on the righthand side of Eq. (15) represents the "temperature" variation that would result under the assumption of diffusive equilibrium. The second term represents the diffusion effect which is independent of ℓ and is relatively more significant for small scale disturbances where the amplitude of the "diffusive equilibrium temperature" becomes small.

Although small scale structures cannot be maintained in the total mass density
(Eq. 10) they prevail in the vertical wind velocity and consequently tend to
maintain the small scale structures in the individual constituents (second
term on the righthand side of Eq. 14) and in the temperature (Eq. 15).

The Equations (10) through (15) are strictly speaking only valid for periods
in the disturbance which are much longer than the characteristic times for
diffusion and advective cooling. For shorter periods the ℓ dependences of course
disappear and transport processes become less effective, a characteristic that
is very significant considering that the duration of storms is variable and that
each storm constitutes an entire spectrum of frequencies.

III. THEORETICAL MODEL

The theoretical model used in our calculations has been described in Mayr
and Volland (1972b). It is essentially a three-dimensional, two-component model
in which heat conduction, advective energy exchange, ion drag, viscosity and diffusion
are considered in a self consistent form. Two versions of the two-component
model are used. One in which the O and N_2 constituents are considered and
which also provides a realistic description of the temperature, and a second
one in which He is considered diffusing through a fictitious constituent with a
mass corresponding to the mean molecular mass of all the other species.
This model provides also an estimate of the "diffusive equilibrium temperature."
To simplify the mathematical analysis perturbation theory is applied and the

latitude and time dependences are described in terms of spherical and Fourier

harmonics respectively.

In our calculations we adopted the same input parameters that have been

used in Mayr and Volland (1972b) except for the height distribution of the heat

input. Cole (1962, 1963, 1971) has shown that Joule heating is an important heat-

ing mechanism during magnetic storms with the maximum of the heat input rate

occuring at altitudes as high as 150 km. We have chosen therefore in our cal-

culations a heat input distribution shown in Figure 3.

IV. MAGNETIC STORM ANALYSIS

To illustrate and verify the effects that have been qualitatively discussed

in Section II we have computed the density, temperature and wind fields for

heat inputs with various latitude structures described in the forms of the

sperical harmonics P_0, P_2, P_4 and P_8. The magnitude of the heat input at the

poles is given in Figure 3. The time period chosen for these calculations was two

days representative of the time scale for the major energy input of a magnetic storm.

Figures 4 and 5 describe the relative amplitudes and phases for the three

constituents N_2, O and He and for the temperatures T_g as well as the mass

density respectively. In both figures the density scales are the same but the

temperature scales are expanded by a factor of twenty.

The distributions for N_2, O and T_g have been derived from the N_2-O model,

and since N_2 and O are the major constituents in the thermosphere the

temperature variations from this model are considered to be realistic. The He

distribution and the "diffusive equilibrium temperature" were derived from the

He model in which the composition of the major constituents was assumed to be

constant with time. n are the orders of the spherical harmonics P_n and since with

increasing n number the structure in the latitudinal variation increases it is ap-

proximately related to the horizontal scale factor ℓ (see Section II) by

$$n \propto \frac{1}{\ell}$$

It is apparent from Figure 4 that the amplitude in N_2 decreases with in-

creasing n in accord with the temperature decrease in Figure 5. The most

drastic decrease occurs between P_0 and P_2 thus demonstrating the importance

of the advective energy exchange associated with the thermospheric circulation

set up in P_2 but not in P_0. Furthermore it can also be seen that the rate of

this decrease slows significantly down at higher wave numbers n. This latter

characteristic was expressed in Eq. 15: The "diffusive equilibrium contribu-

tion" in the temperature decreases with increasing n (or decreasing horizontal

scale ℓ) but the diffusion effect upon temperature and major constituent remains

essentially independent of n (for n > 0) and thus becomes dominant at greater

wave numbers.

The importance of the diffusion effect for the minor constituents O and He

is evident in Figure 4. In the globally uniform component P_0 the diffusion

process can only be excited by the one dimensional thermal expansion and

contraction of the thermosphere. Combined with the relatively large temperature effect, diffusion is thus rather unimportant. This is apparent in both constituents O and He (solid lines) which vary more or less in phase with the temperature above their isopycnic levels at 175 and 300 km respectively with their amplitudes being essentially proportional to their mass at exospheric heights.

For the nonuniform components P_2 through P_8 the thermospheric circulation is significantly involved in the diffusive redistribution of the minor constituents which, combined with the relatively small temperature effects, becomes very important. Thus both constituents are by almost 24 hours (180°) out of phase with the temperature and the N_2 concentration, implying that the minor species decrease at times when N_2 and T_g increase, in agreement with our earlier results (Mayr and Volland, 1972a). It is also apparent that this diffusion effect is essentially independent of n and thus contributes to the above discussed diffusion effect in the temperature.

There are, however, some significant differences between the He and O distributions which bear upon the differences in the mass and abundance of both species. Accordingly, the diffusion effect is much less pronounced for O than for He. In addition the temperature effect is more important for O than for He and thus compensates the diffusion effect in O at higher altitudes. The consequence of the latter is that the amplitude in O initially decreases above 200 km with its phase gradually shifting toward the temperature phase at greater heights.

After going through an isopycnic level at exospheric heights the amplitude in

O again increases with height and this constituent begins to vary, although greatly

damped, more or less in phase with the temperature and the N_2 concentration.

The height of this isopicnic level depends on the temperature amplitude. Thus

it is lowest for P_2 (300 km) (and still lower of course for P_0 (175 km)) and it in-

creases to altitudes above 450 km for P_8. For He with the weaker temperature

and stronger diffusion-effect such an inversion does not take place (except for

P_0) and its 180° phase difference with N_2 and T_g remains intact throughout the

thermosphere.

It is interesting to note the rather complex behavior in the phase relations

between the various physical parameters. As n increases the phases of the mass

density and "diffusive equilibrium temperature" are advanced to earlier times at

exospheric heights. This phase shift is particularly large between P_0 and P_2

when for n > 0 advection becomes very important thereby reducing

substantially the characteristic time for the energy exchange. This latter

mechanism is also the reason for the initial phase shift between the P_0 and P_2

components in the temperature and the N_2 concentration. With increasing wave

numbers n,the phases in atomic oxygen and helium are also shifted toward

earlier times but for n > 0 the N_2 and T_g phases are advancing toward later

times. With increasing n the diffusion process leads to an increasing separation

of the phases of the individual constituents away from the phase of the mass density

and "diffusive equilibrium temperature." Thereby, the heavier constituent and

the temperature go into one and the lighter constituents go into the other direction,

indicating a sort of diffusive separation in time space.

Finally, it is shown in Figure 5 that between P_0 and P_8 the amplitudes of

the mass density and diffusive equilibrium temperature decrease by about a

factor of 100 at exospheric heights in agreement with the n dependence in Eq. 10

and with our earlier results from an analytical model (Volland and Mayr, 1971).

It is therefore understandable that the satellite drag data, which measure the

mass density, can only observe the global components in the magnetic storm

response of the thermosphere quite contrary to the composition and temperature

measurements which should be capable of "recognizing" the local character of

the disturbance.

Figure 6 shows the amplitudes and phases for the vertical and meridional

transport velocities of the N_2 constituent. For n = 0, that is for the global com-

ponent, the horizontal velocities are of course zero. However with increasing

n the meridional velocity decreases and the vertical velocities remain

essentially constant, both features being consistent with the relations (12)

and (13). The latter characteristic is responsible for the fact that the

diffusion effect is nearly independent of n as has been pointed out before.

For n = 0 the vertical velocity is smaller than that for n > 0 in the lower ther-

mosphere where diffusion is important, however, it is greater at higher altitudes

thus accounting for the larger temperature amplitude in P_0 and for the lack of horizontal mass transport. It can be seen that the meridional transport velocities change their direction at about 150 km blowing away from the heat source above this level and blowing toward the heat source below it with the center of the circulation apparently occuring near the height for the energy input maximum.

The vertical transport velocities for atomic oxygen and helium are up to 30% higher than those of the major constituents in the lower thermosphere. Since all the vertical transport velocities are almost in phase there, this implies that a downward drag force is applied with its maximum value near the time of the maximum energy input, and this is consistent with the depletion effect of the O and He during disturbed conditions.

V. MAGNETIC STORM SYNTHESIS

To visualize the magnetic strom response in the thermosphere we constructed a heat source in the form

$$Q = \sum_{n=1}^{3} \cos(n\omega t) \sum_{m=0}^{8} Q_{nm} P_m(\theta)$$

for $\omega = 2\pi/\tau$ with τ being the time period of two days, and for m = 0, 2, 4, 6, 8 thus describing a heat source that is symmetrical with respect to the equator. Figure 7a shows the distribution of the heat input rate at the time of the input

maximum and Figure 7b shows the time variation of the heat source in the auroral zones. The shape for the height variation of the heat input is the same that was shown in Figure 3. The values in Figure 7 were taken from 140 km. Since we restrict ourselves to a rather limited number of harmonics the input distribution is not too realistic in particular with regard to the waves at low latitudes and before and after the storm, and they should be ignored in the interpretation of our results.

In the following we shall present our results in the form of contour plots in time-latitude frames. To facilitate the comparison with the heat input distribution we show in Figure 8 again the heat source in a contour plot. The time scale is chosen such that the heat input maximum occurs at 00 UT. To emphasize that some of the structures before and after the storm and at low latitudes are unrealistic we show them in thin lines.

Figures 9a through 9e show at 200 and 450 km the distributions of the N_2, O and He constituents as well as those of T_g and the mass density ρ respectively. The contour densities were scaled with a factor s, normalized to 1 for N_2 at 450 km, such that in each figure the number of contours is approximately constant. This serves the purposes to provide the optimum information on the temporal and latitudinal structure and to provide a means of assessing the magnitudes of the variations by comparing the scale factors s. For the actual magnitudes of the variations the numerical values associated with each contour have to be considered, and in evaluating these numbers it has to be kept in mind that they

represent relative variations to be superimposed upon the time average and globally uniform component of the thermosphere.

From Figures 9a through 9c the disparity in the magnetic storm response of the various atmospheric constituents becomes apparent. The N_2 concentration increases within the auroral zone where most of the energy is deposited, and this behavior is there in accord with the temperature enhancement shown in Figure 9d. The time and latitude scales in the variations of N_2, however, are substantially larger than those in the heat source (Fig. 8). This is particularly apparent from the lack of structure at low latitudes and after the storm, and from the elongation of the N_2 bulge toward the poles and toward later times.

In contrast, O in Figure 9b is shown to decrease in the auroral zone at 200 km with some trend to increase at low latitudes. While the latitudinal variations reflect the structure in the heat source, the time scale in the response of O is due to the long diffusion time even larger than that in N_2. Completely different are the characteristics in the distribution of O at 450 km. Here during the storm atomic oxygen peaks at the poles and decreases gradually toward the equator resembling not at all the rather localized heat input into the auroral zone. The time scale at 450 km is at a given latitude, however, much narrower than at 200 km with the density maximum progressing to later times as one moves away from the auroral zone. A comparison between the storm time variations in N_2 and O at 450 km reveals that N_2 increases by about a

factor of 4 between equator and auroral zones while O increases only by about

20% in this latitude range in substantial agreement with the observations of

Taeusch et al., 1971 and with our earlier results (Mayr and Volland, 1972a).

With regard to the phase relations it can be seen that in the auroral zone at

450 km O peaks at about 2^{00} UT followed by T_g at 3^{00} UT and N_2 at 3^{30} UT, a

behavior basically very similar to the response sequence in the diurnal varia-

tions of the composition (Mayr and Volland 1972c).

Helium which is even more affected by the diffusion process than O is also shown

to decrease in the auroral zone. The amplitudes smaller than or equal to

−1 are of course unrealistic thus reflecting upon the limitations in the perturba-

tion approach. However, apart from that our He model is also for other reasons

rather crude since thermal diffusion has been neglected and since by consider-

ing only two components the temperature variations in the He model are un-

realistically small. A proper description of He would require a model in

which the diffusion and energy transport of the three constituents He, O and N_2

are considered in a self consistent form. Nevertheless, our results indicate

that magnetic storms can induce a substantial reduction in He at times when the

N_2 concentration is enhanced. Since the temperature is not very effective for

He, it cannot cancel the diffusion effect (as for O) and hence the He decrease in

the auroral zone and the enhancement at low latitudes remain intact throughout

the thermosphere.

Figure 9e finally shows the response in the mass density ρ which is observed in the satellite drag data. Both at 200 and at 450 km the latitudinal variations in ρ during the storm are relatively insignificant and do not at all reflect the local heat input into the auroral zone. In particular, it is apparent that the global response in ρ is relatively significant (60%) when compared with the 40% increase between equator and pole during the storm at 450 km. This predominance in the global component - which is even more pronounced at 200 km-confirms thus our earlier conclusions (Volland and Mayr, 1971) and appears to be in substantial agreement with the satellite drag data. The maximum in the mass density at 450 km occurs near 2^{00} UT at high latitudes and shifts toward 8^{00} UT at the equator, again in basic agreement both with Volland and Mayr (1971) and with the average time lag of 6^{00} hrs deduced from satellite drag data (Jacchia et al. 1967).

Figure 10 illustrates the difference between the actual computed gas temperature and a sort of "effective temperature" which we deduced under the assumption of diffusive equilibrium from the variations in the mass density at 450 km. The latter "temperature is equivalent to the one that has been inferred from the satellite drag data. The delay of six hours chosen for this comparison corresponds approximately to the response time of the global component in the mass density. For Figure 10 the relative temperature variations were converted into absolute values with a pre-storm temperature of 1000°K. It is then apparent that the gas temperature increases only slightly at the equator but

increases by about 250°K from the equator toward the auroral zone where a pronounced peak develops. In contrast the "effective temperature" increases by 120°K at the equator reflecting upon a relatively strong global component and increases by only 40°K from the equator toward the pole where an elongated "temperature" bulge develops. While the magnetic storm response in the mass density can thus be reconciled with the variations in the composition as observed on OGO-6 the temperature derivation from the satellite drag data can definitely not be justified.

Figure 11 shows contour plots for the O/N_2 ratio at 200 km deduced from our model. This ratio is an important parameter for the magnetic storm response of the ionosphere since the electron density at and below the F_2 peak varies proportional to the ionization rate, which depends on O, and inversely proportional to the ion-molecule charge transfer rates, which depend on N_2 and O_2. Our results show that the electron density in the F_2 region could decrease up to about a factor of three at high and mid latitudes and slightly increase at low latitudes, a result which verifies the hypothesis of Seaton (1956), Duncan (1969), Chandra and Herman (1969), and Obayashi and Matuura (1972), who postulated this kind of composition changes in interpreting the magnetic storm response of the ionosphere.Obayashi and Matuura (1972) also suggested that the composition effect could be induced by the thermospheric circulation. However, in addition to these composition changes which influence the ionpsphere through the ion chemistry, at least three other features in the

magnetic storm response of the neutral atmosphere could be of importance for the ionosphere. These are (a) the nearly global increase in the thermospheric density which will decrease the ionospheric diffusion coefficient and thus enhance the electron density and height of the F_2-maximum (b) the effects of the changing composition and temperature upon the energetics of the ionosphere which are probably rather complex when considered in conjunction with the processes of non local heating and (c) the effects of thermospheric winds (Kohl and King (1967), Obayashi (1972)) which obtain during storms an additional equatorward component, shown in Figure 12, that would tend to decrease the electron density below the F_2 maximum and to enhance it at and above the F_2 peak.

Finally, Figures 12 and 13 show the meridional and vertical components of the velocity field for atomic oxygen. Our results show that below 250 km, where oxygen is the minor constituent, the differences for the vertical transport velocities of O and N_2 are less than 30% while the horizontal transport velocities for both constituents are essentially identical. For this reason we consider the velocities in Figures 12 and 13 to be representative of the wind field. From these figures it is then apparent that during disturbed conditions a large scale circulation is set up with air rising in auroral latitudes and descending at low latitudes. The meridional velocities attain thereby values as high as 150 m/sec at mid latitudes, sufficient to affect significantly the F_2 region ionization. The meridional velocity is shown in particular to increase gradually toward mid

latitudes thus reflection the predominance of the large scale components (see the ℓ dependence in Eq. 12). In contrast, the vertical velocity component tends to be independent of ℓ (see Eq. 13) and hence reveal the details in the heat input distribution to a much greater extent, the latter being also the reason for the abrupt changes in the neutral composition as discussed before.

VI. SUMMARY AND CONCLUSION

Considering simple dimensional relations, some of the most important characteristics in the magnetic storm response of the thermosphere were qualitatively discussed thereby showing that the diffusive redistribution of atomic oxygen can have effects upon the temperature structure. A quantitative three–dimensional model of the thermosphere dynamics was then presented. In this model energy and diffusive mass transport associated with the magnetic storm–induced thermospheric circulation are considered in a self-consistent form. Our results show that these processes indeed play a major role in the thermosphere and thus account for a number of composition, temperature and mass density phenomena which are observed in the satellite drag data and in the neutral composition measurements on OGO-6. In particular the model describes

(a) the relatively steep temperature enhancement toward high latitudes during disturbed conditions,

(b) the depletion effects in atomic oxygen and helium coincident with the temperature increase,

(c) the negligibly small latitudinal variation in atomic oxygen in the presence of a significant increase in N_2 and a similarly drastic decrease in He toward the auroral zones at 450 km,

(d) the gradual increase in the mass density ρ between equator and pole superimposed upon a relatively strong global enhancement in ρ during disturbed conditions,

(e) the gradual phase shift in the response time of ρ from 2 to 8 hrs between pole and equator and

(f) the phase sequence between the individual atmospheric parameters with the maximum in O occuring closest to the time of the energy deposition followed by the maximum in T_g and that of N_2 in the auroral zone at 450 km.

In producing a temperature increase of about 400°K which corresponds to the storm time condition specifically described here, an energy input rate comparable to that due to the EUV was required. We adopted thereby a height distribution for the heat input which we considered to be representative of Joule heating (Cole, 1971).

Although it appears that our model can describe some of the major features in the magnetic storm response of the thermosphere, it must still be qualified as a first order approach toward a self-consistent treatment of the diffusion and energy transport mechanisms in the thermosphere dynamics. The application

of perturbation theory and the restriction to the first few harmonics which were considered independently characterize our approximations. Furthermore we restricted ourselves to a two component model which is not entirely adequate for He. Apart from these limitations,which were imposed for mathematical convenience, there are a number of processes which have not yet been considered. Ion drifts (associated with the magnetic storm induced electric fields) which couple momentum into the neutral atmosphere (Cole, 1971), the feedbacks from the magnetic storm response in the ionosphere and the effects of particle precipitation which deposit their energy presumably within the lower thermosphere and mesosphere (Rees 1972) are just a few of the mechanisms to be further investigated.

VII. REFERENCES

Chandra, S. and J. R. Herman, F region ionization and heating during magnetic storms, Planet. Space Sci., 17, 841, 1969.

Cole, K. D., Joule heating of the upper atmosphere, Aust. J. Phys., 15, 223, 1962.

Cole, K. D., Joule heating of the ionosphere over Halley Bay, Nature, Lond. 199, 444, 1963.

Cole, K. D., Electrodynamic heating and movement of the thermosphere, Planet. Space Sci., 19, 59, 1971.

Duncan, R. A., F region seasonal and magnetic storm behavior, J. Atm. Terr. Phys., 31, 59, 1969.

Jacchia, L. G., Two atmospheric effects in the orbital acceleration of artificial satellites, Nature, 183, 526, 1959.

Jacchia, L. G., J. Slowey and F. Veriani, Geomagnetic perturbations and upper atmospheric heating, J. Geophys. Res., 72, 1423, 1967.

Kohl, H. and J. W. King, Atmospheric winds between 100 and 400 km and their effects on the ionosphere, J. Atm. Terr. Phys., 29, 1045, 1967.

Mayr, H. G. and H. Volland, Temporal variations in the thermospheric composition, EO5, 51, 789, 1970.

Mayr, H. G. and H. Volland, Magnetic storm effects in the neutral composition, Planet, Space Sci., 20, 379, 1972a.

Mayr, H. G. and H. Volland, Theoretical model for the latitude dependence of the thermospheric annual and semiannual variations, NASA-Document X-621-72-235, J. Geophys. Res., in press 1972b.

Mayr, H. G. and H. Volland, Two component model of the diurnal variations in the thermospheric composition, NASA Document X-621-72-233, J. Atm. Terr. Phys., in press 1972c.

Obayashi, T. and N. Matuura, Theoretical model of F-region storms, Proc. Solar Terr. Phys., 4, 199, 1972.

Obayashi, T., World wide electron density changes and associated thermospheric winds during an ionospheric storm, Planet. Space Sci., 20, 511, 1972.

Rees, M. M., private communication, 1972.

Roemer, M., Geomagnetic activity effect derived from Explorer 9 data, Phil. Trans. Roy Soc. London, A, 262, 184, 1967.

Seaton, M. J., A possible explanation of the drop in F-region critical densities accompanying major ionospheric storms, J. Atm. Terr. Phys., 8, 122, 1956.

Taeusch, D. R., G. R. Carignan and C. A. Reber, Neutral composition variation above 400 kilometers during a magnetic storm, J. Geophys., Res., 27, 8318, 1971.

Volland, H and H. G. Mayr, Response of the Thermospheric density to auroral heating during geomagnetic disturbances, J. Geophys. Res., 76, 3764, 1971.

VIII. FIGURE CAPTIONS

Figure 1. Schematic diagram for the physical processes that influence the

temperature, composition and wind field of the thermosphere.

Figure 2. Schematic diagram for the physical properties of the thermosphere

which affect the temperature, composition and wind field.

Figure 3. Height distribution for the heating rate considered to be representa-

tive of Joule heating (Cole, 1971).

Figure 4. Computed relative amplitudes and phases for N_2, O and He at the

poles associated with the spherical harmonics P_0, P_2, P_4 and P_8. The

heating rate distributions used in the calculations had the same latitude

dependences with polar amplitudes equal to the input distribution in

Figure 3.

Figure 5. Same as in Figure 4 but for the mass density, T_g and the "diffusive

equilibrium temperature." The latter was derived under the assumption

that the mean molecular mass is time independent which corresponds only

approximately to the assumption of diffusive equilibrium.

Figure 6. The same as in Figure 4 but for U and W. While the form in the

latitudinal variations of W corresponds again to P_0, P_2, P_4, and P_8, those

for U are different. They are in particular $\sin \theta \, P_1$, $\sin \theta \, (P_3 + 3/7 \, P_1)$

and $\sin \theta \, (P_7 + 11/15 \, P_5 + 7/15 \, P_3 + 3/15 \, P_1)$ corresponding to the heat

input distributions with P_2, P_4 and P_8 respectively.

Figure 7. Global energy input distribution at 140 km. Figure 7a shows the latitude dependence at 00 UT when the maximum occurs. Figure 7b shows the temporal variations of the heat input in the auroral zone. The wave structures before and after the storm and at low latitudes are of no significance. They are merely a manifestation of the limited numbers of harmonics used in the magnetic storm synthesis.

Figure 8. Contour plots of the energy distribution at 140 km for the magnetic storm disturbance.

Figures 9a through 9e. Contour plots of the relative variations in the magnetic storm response of N_2, O, He, T_g and ρ calculated for 200 and 450 km with the energy input distribution defined in Figures 3, 7 and 8.

Figure 10. Computed gas temperature (solid line) in comparison with an "effective temperature" (dashed line) deduced from the mass density under the assumption of diffusive equilibrium.

Figure 11. Contour plots of the relative variations in the magnetic storm response of the O/N_2 ratio of 200 km a parameter which is significant for the ionosphere.

Figure 12. Contour plots of the meridional component in the transport velocity of O. Since the difference between the transport velocities of O and N_2 are negligible below 250 km this velocity is considered to represent the wind velocity.

Figure 13. Contour plots of the vertical component in the transport velocity of

O. The difference with the corresponding component in N_2 can be 30% and

thus the values in this figure represent only approximately the wind

component.

THERMOSPHERE DYNAMICS
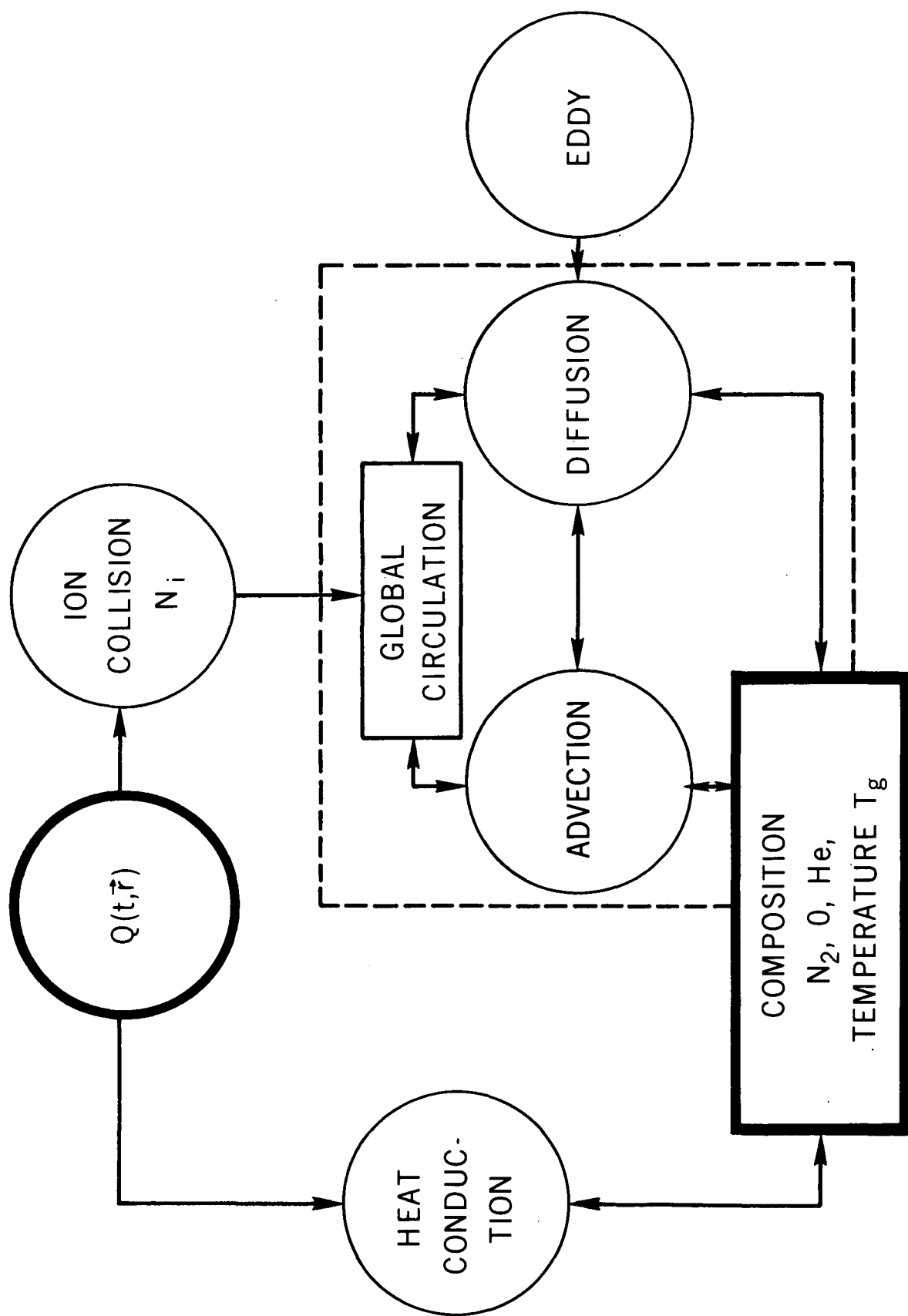
Figure 1

DYNAMIC PROPERTIES
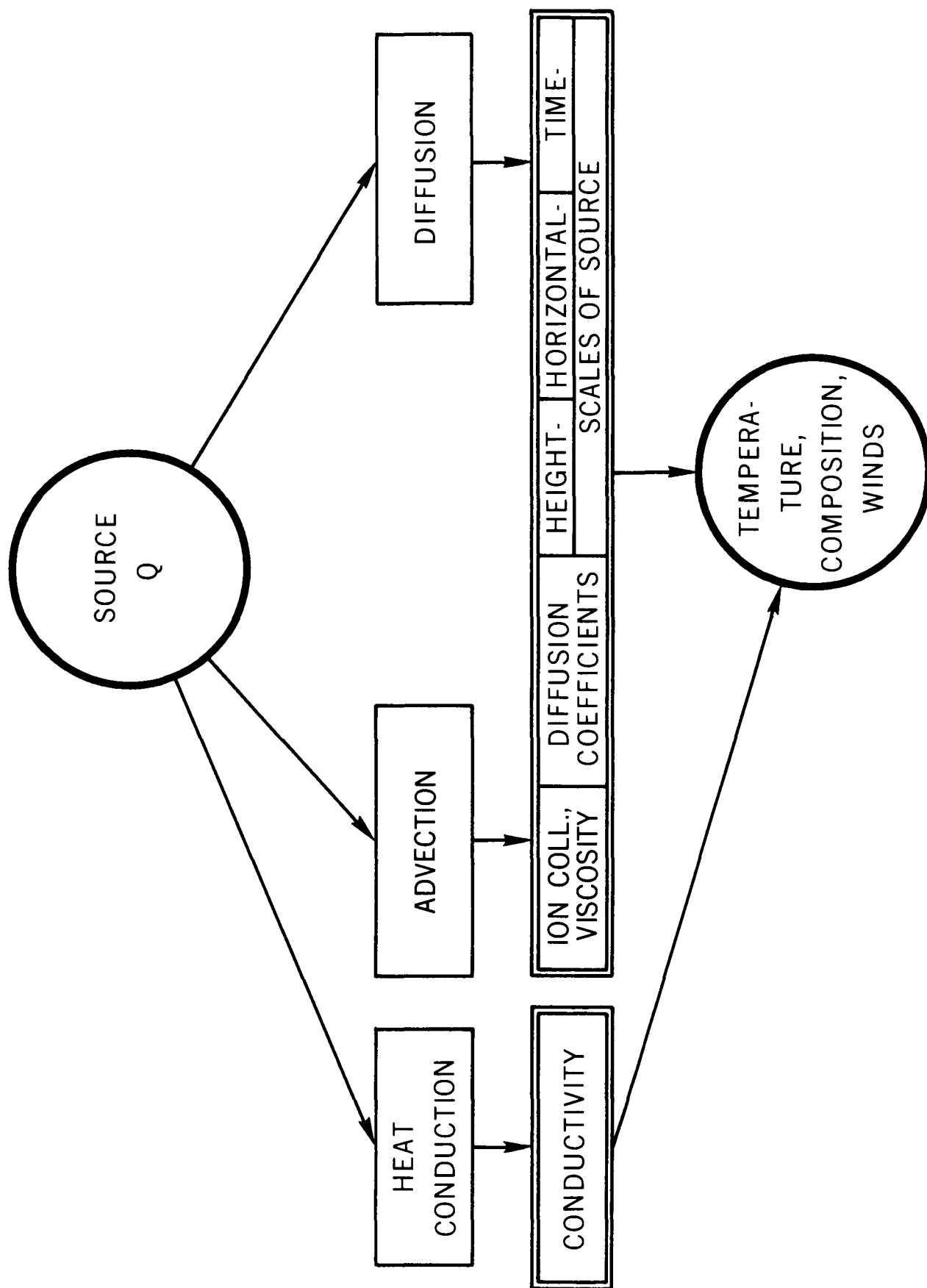
Figure 2

ENERGY INPUT
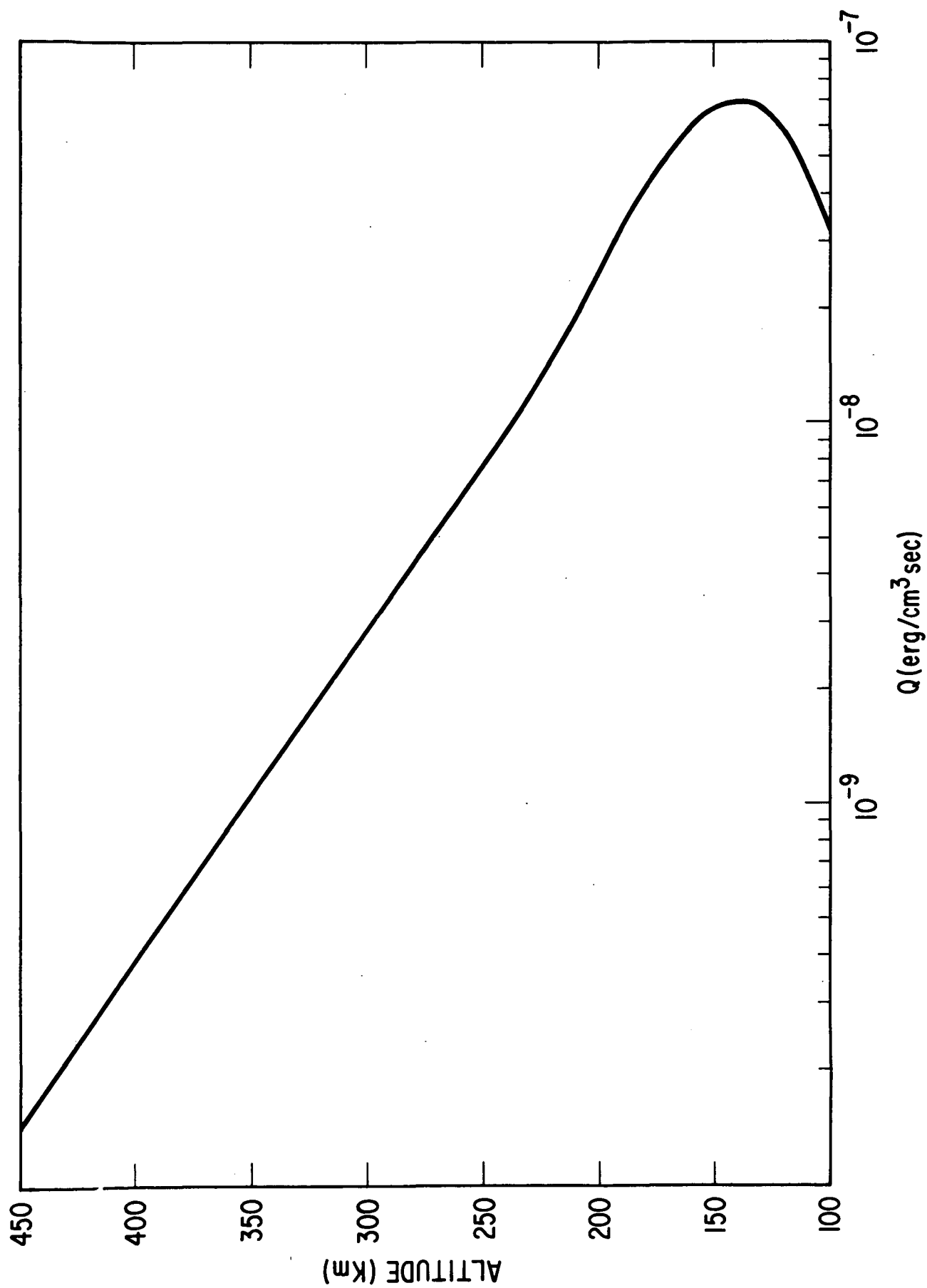
Figure 3
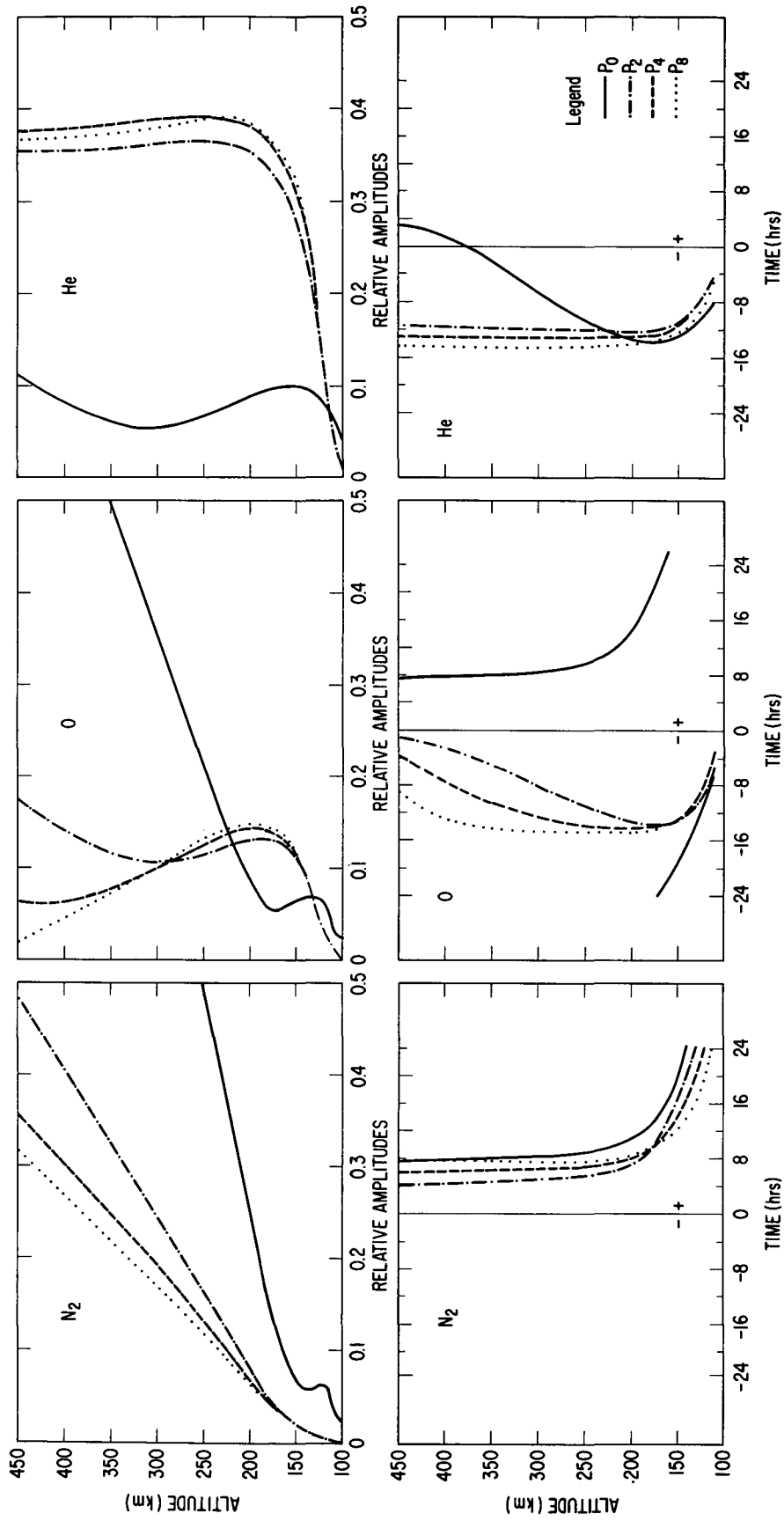
Figure 4
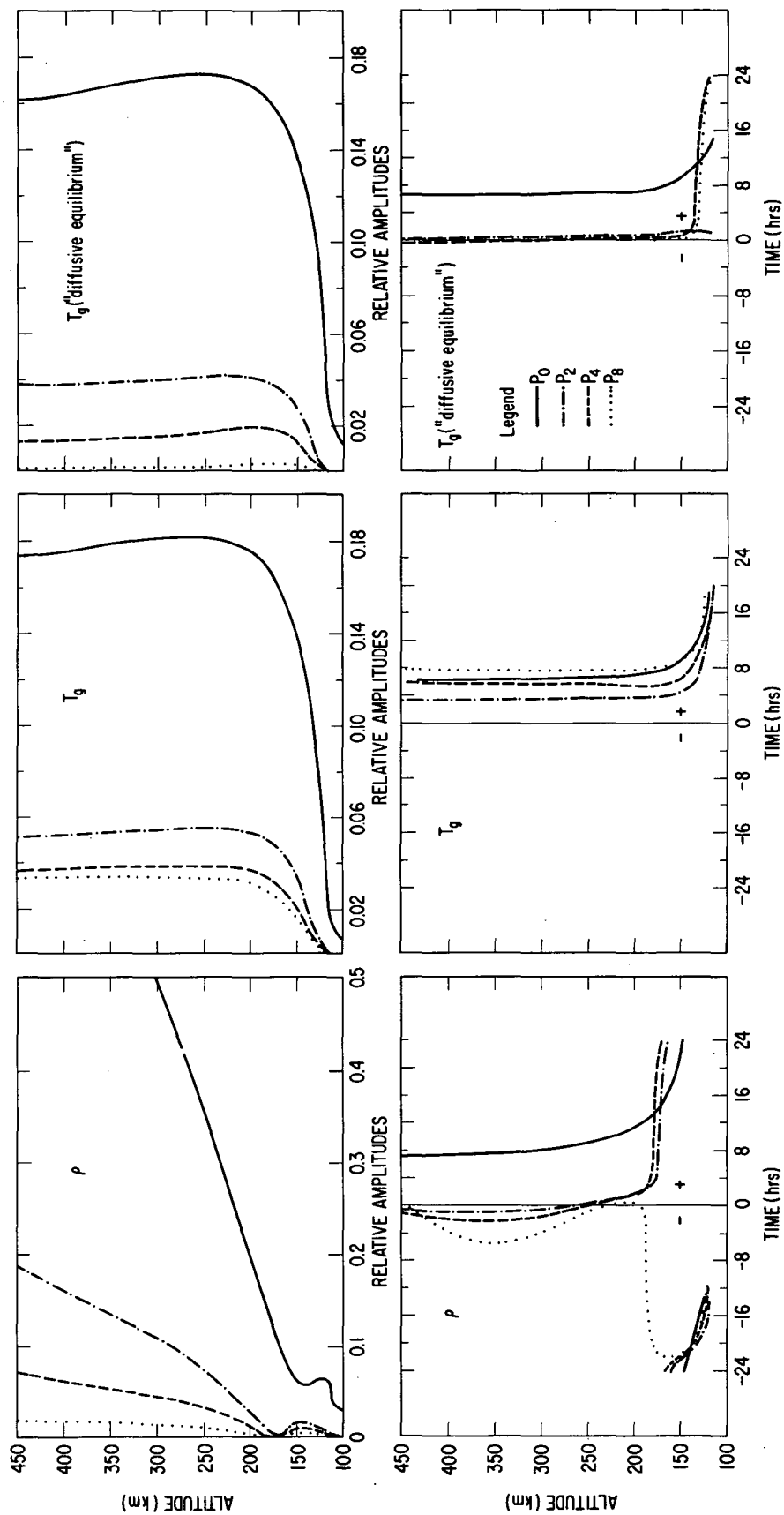
Figure 5
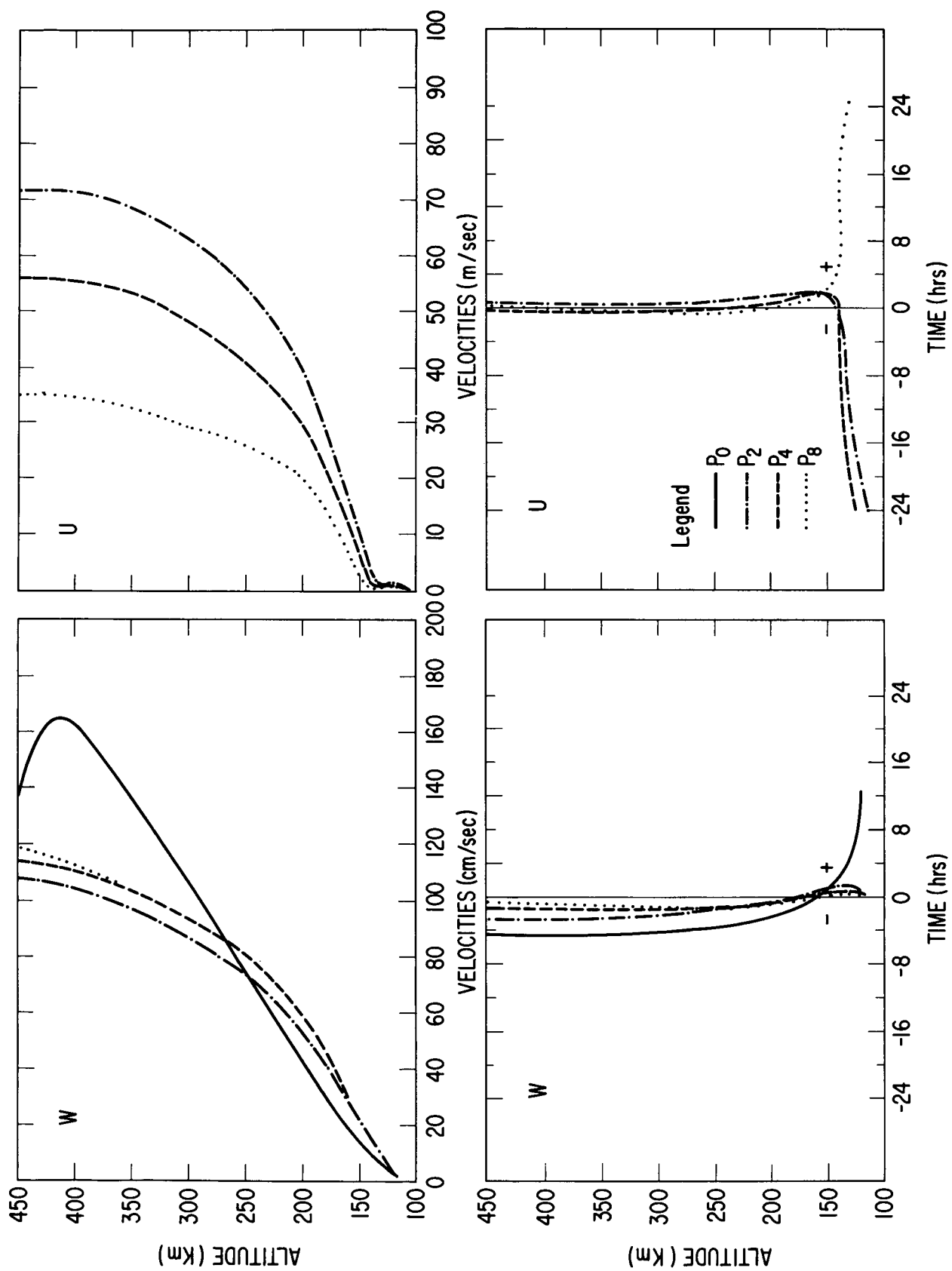
Figure 6

ENERGY INPUT

Figure 7

ENERGY INPUT x10⁸ erg/cm³sec AT 140 Km
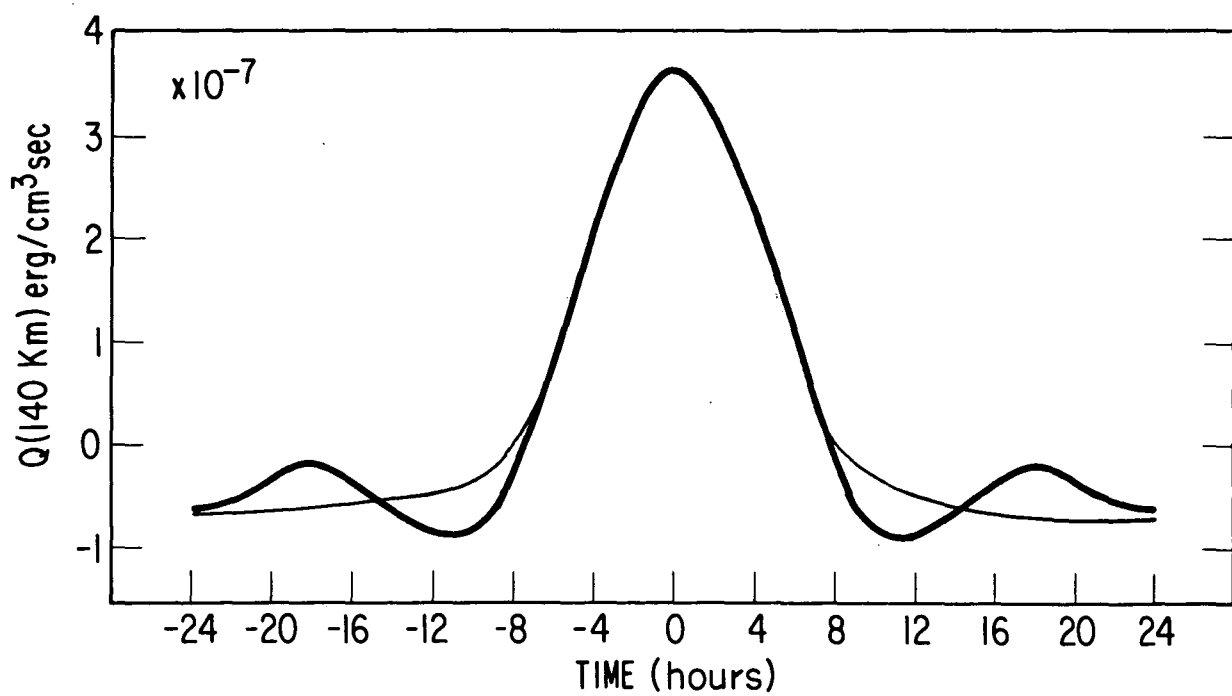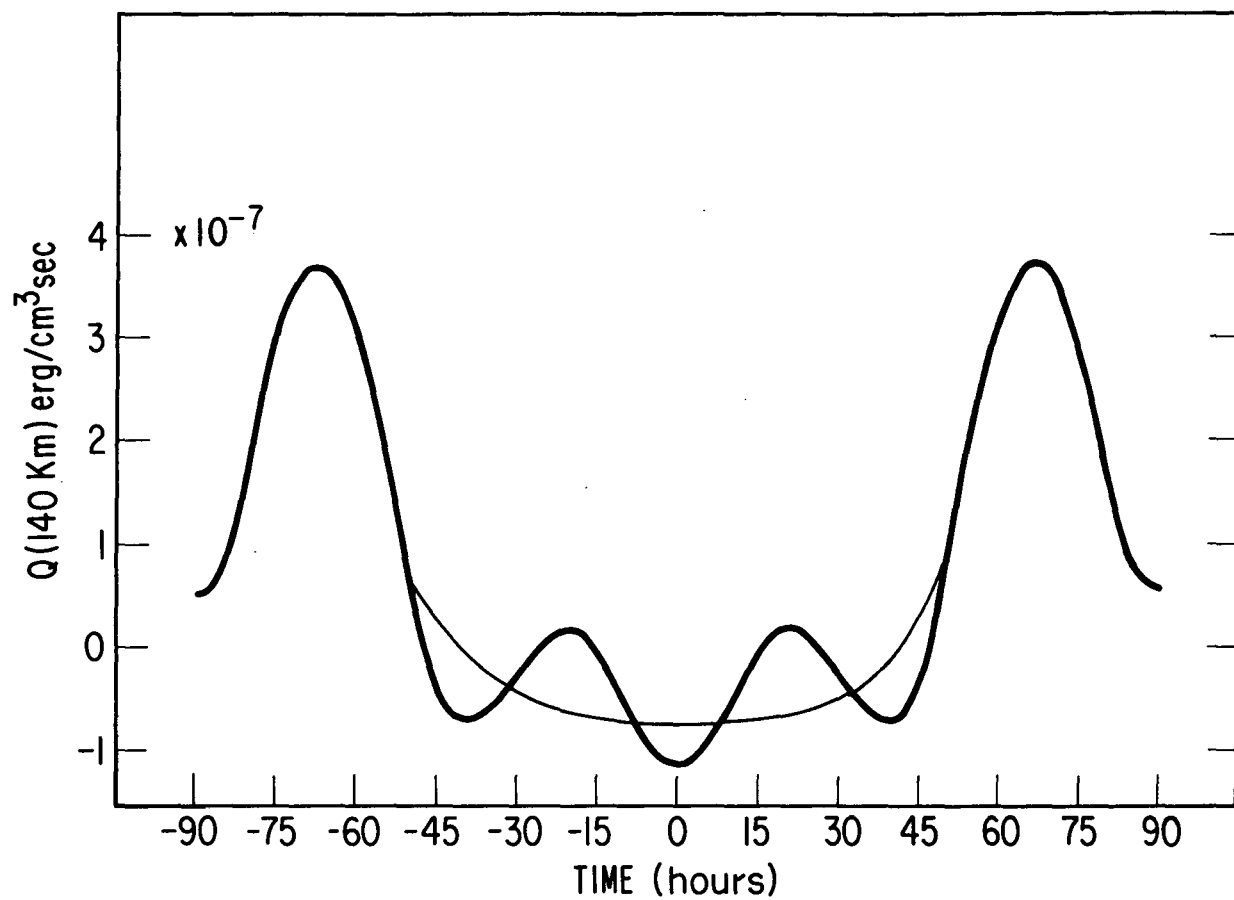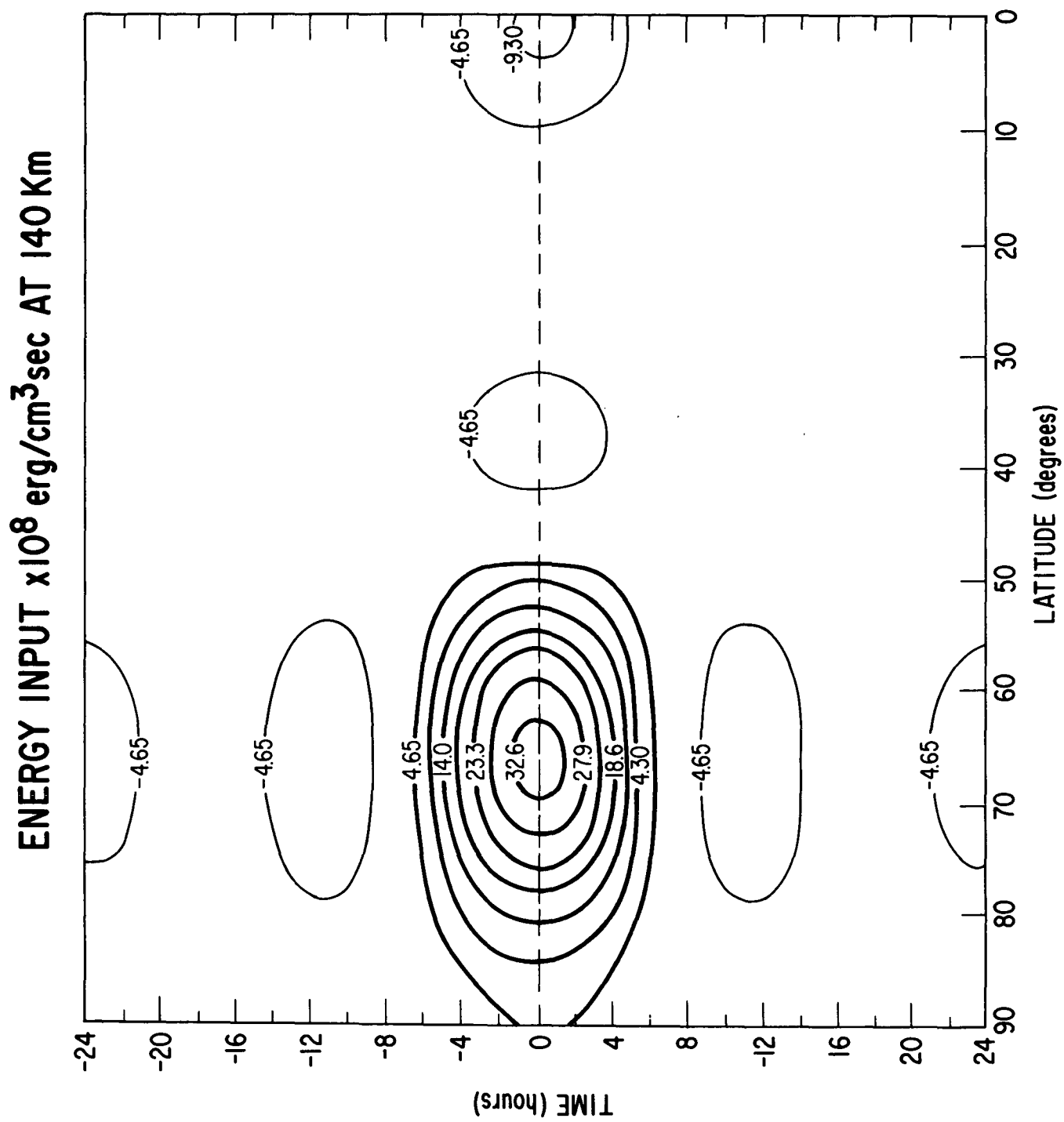
Figure 8

N₂ CONCENTRATION
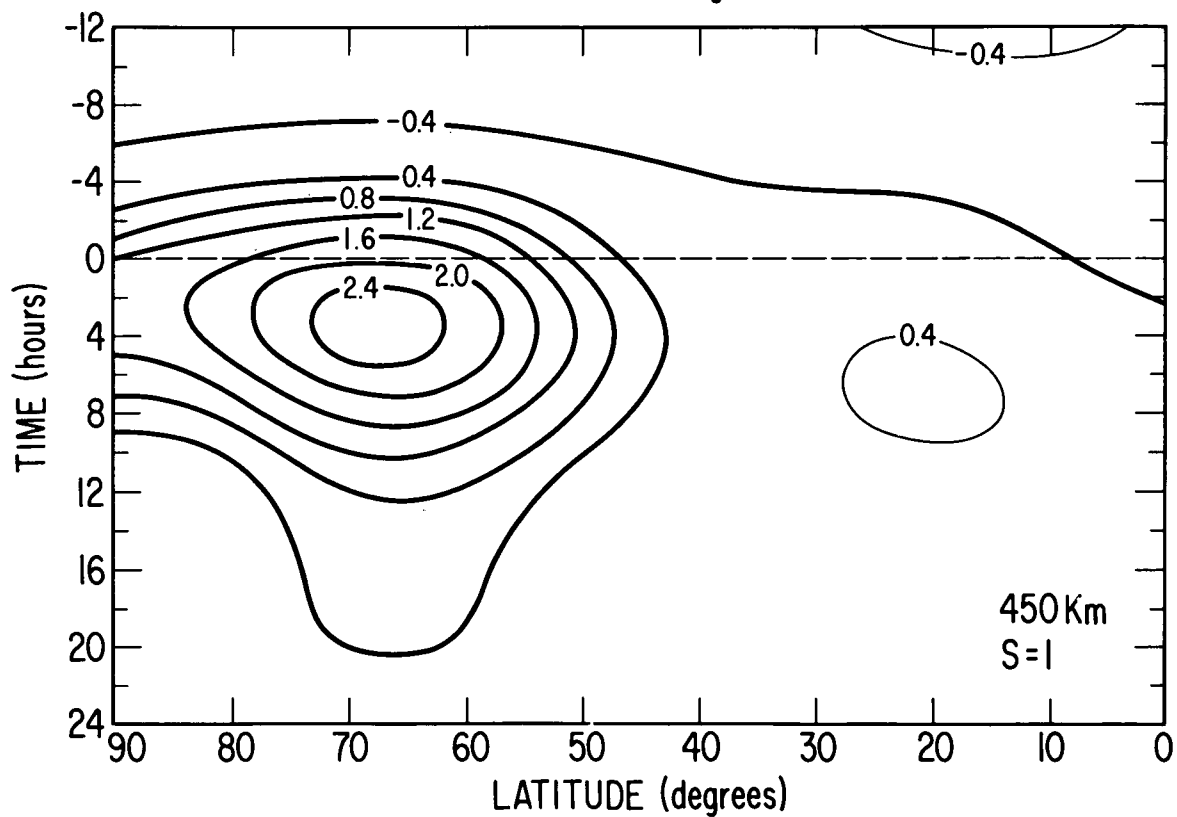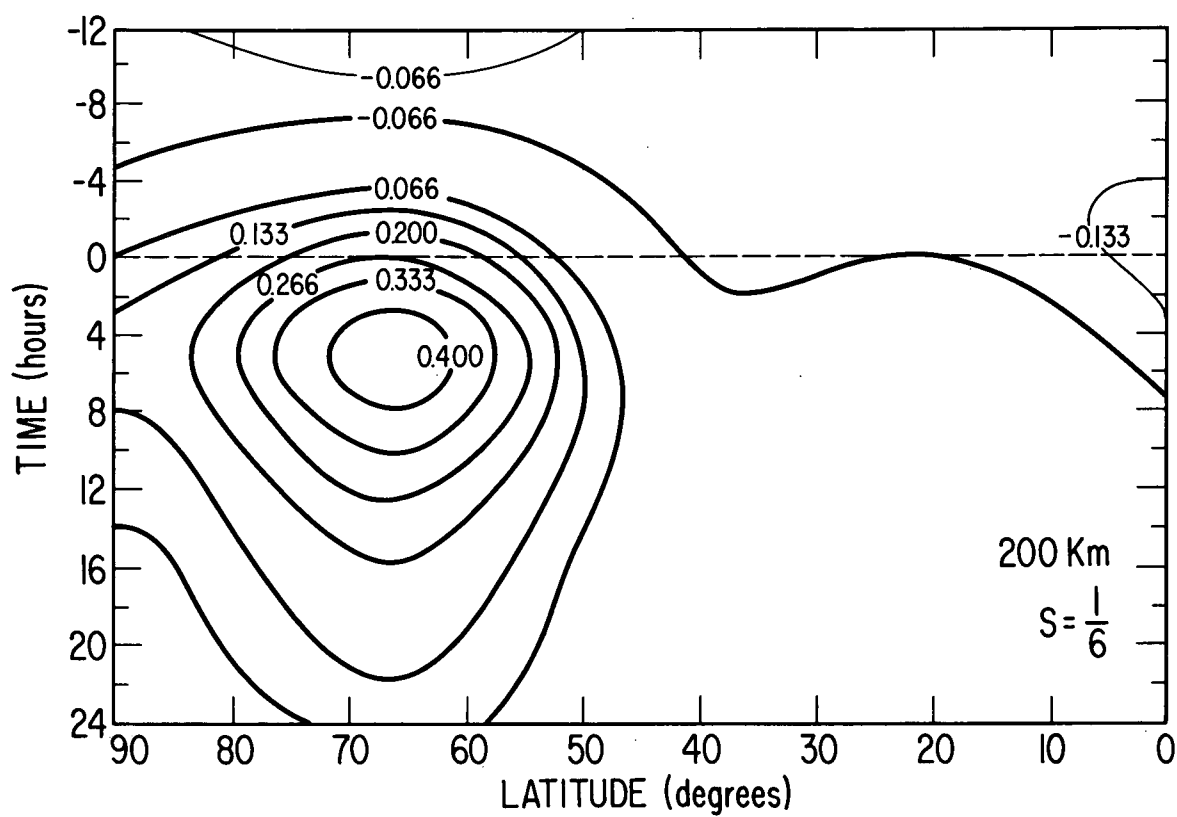
Figure 9a

OXYGEN CONCENTRATION
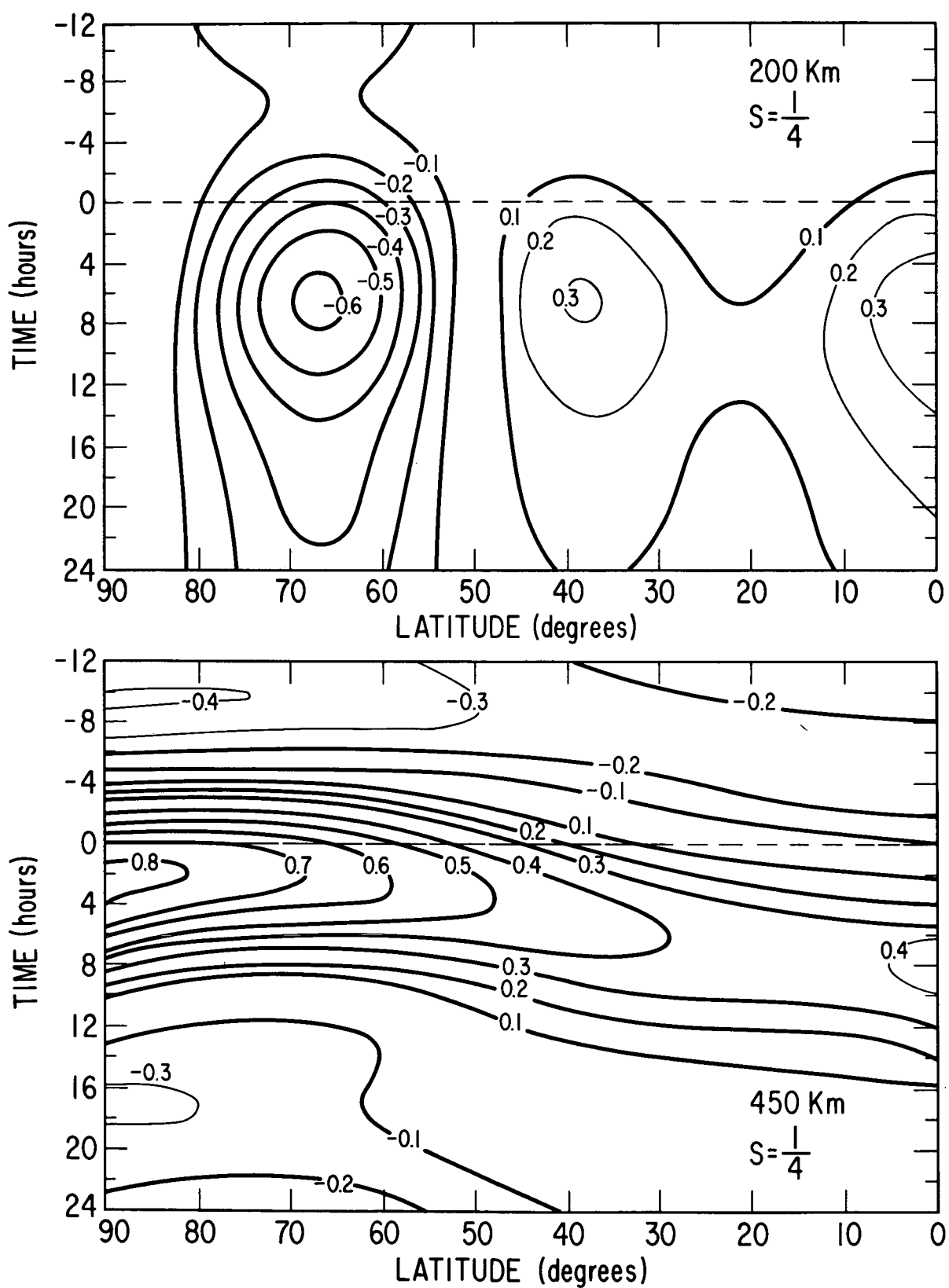
Figure 9b

He CONCENTRATION
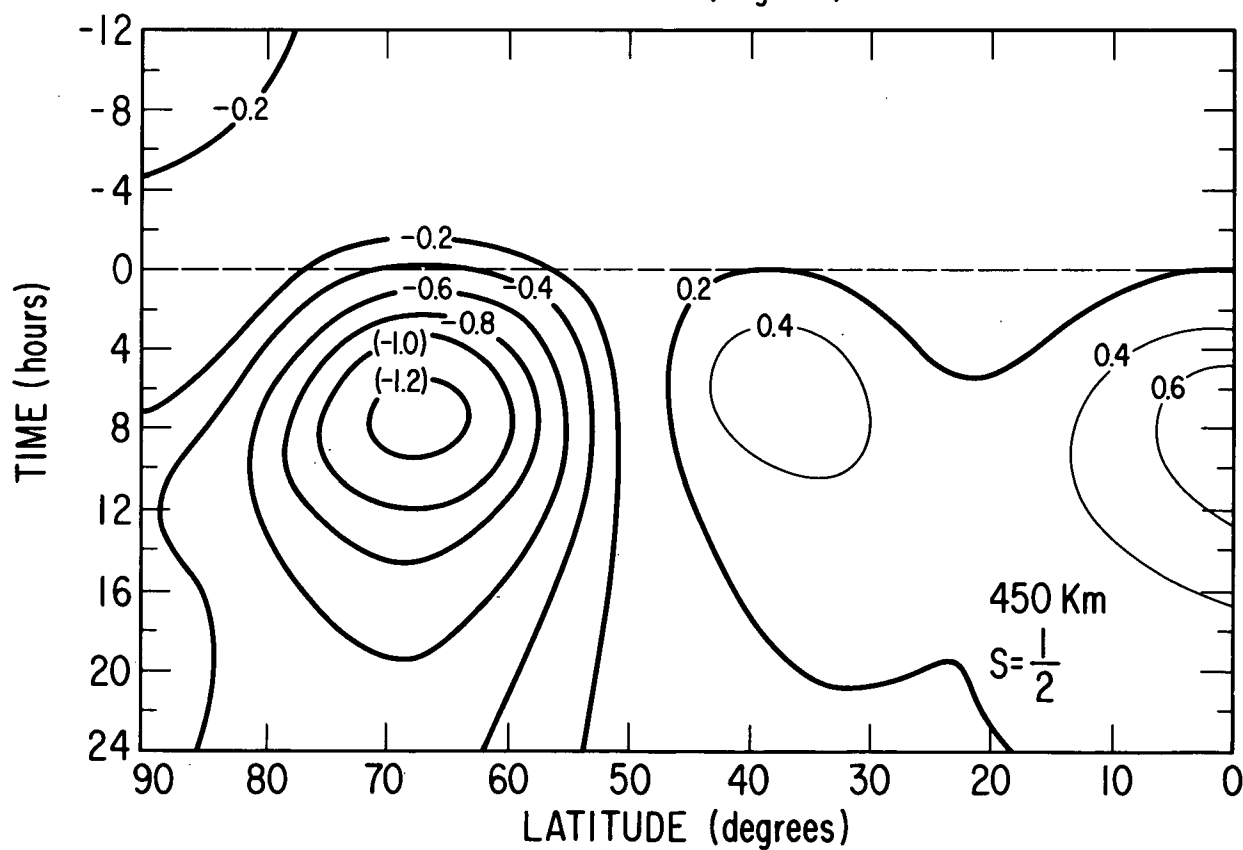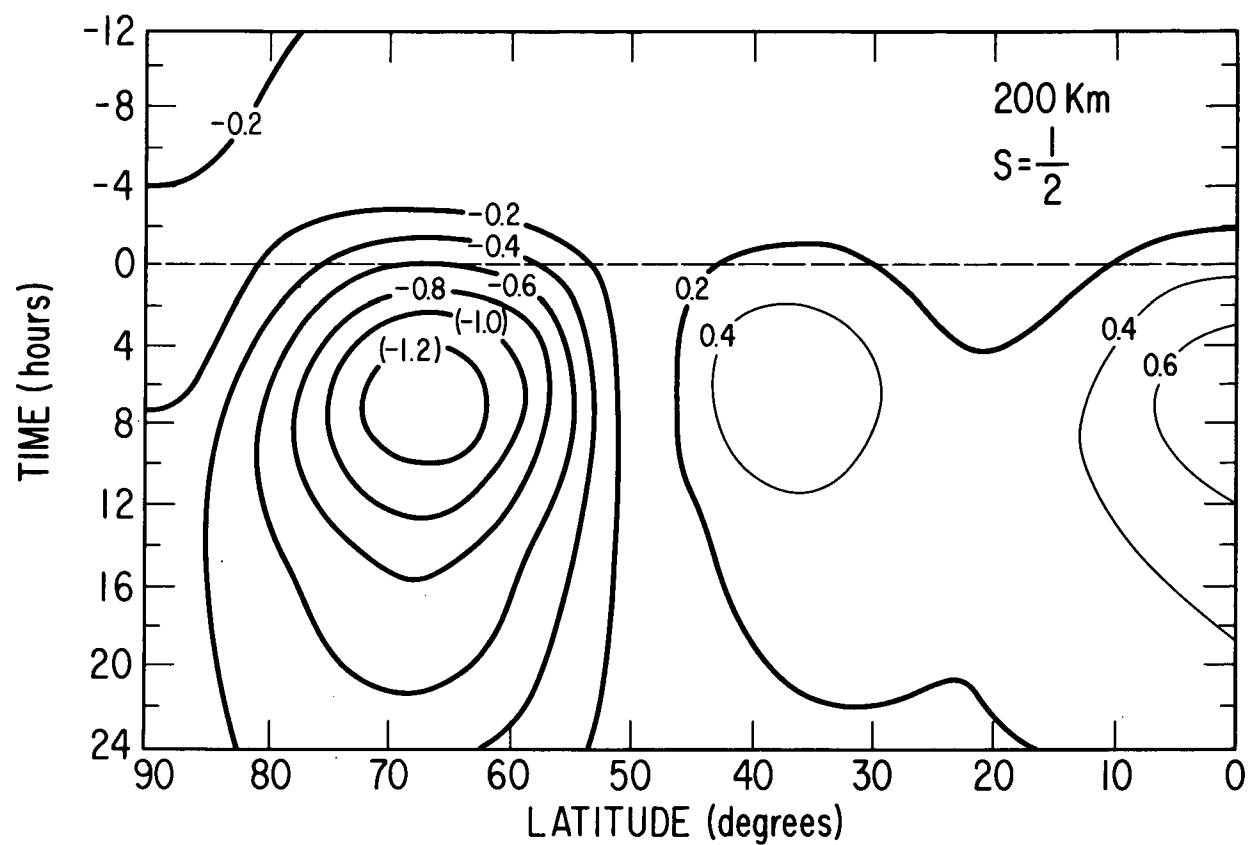
Figure 9c

TEMPERATURE T$_g$

Figure 9d

MASS DENSITY ρ
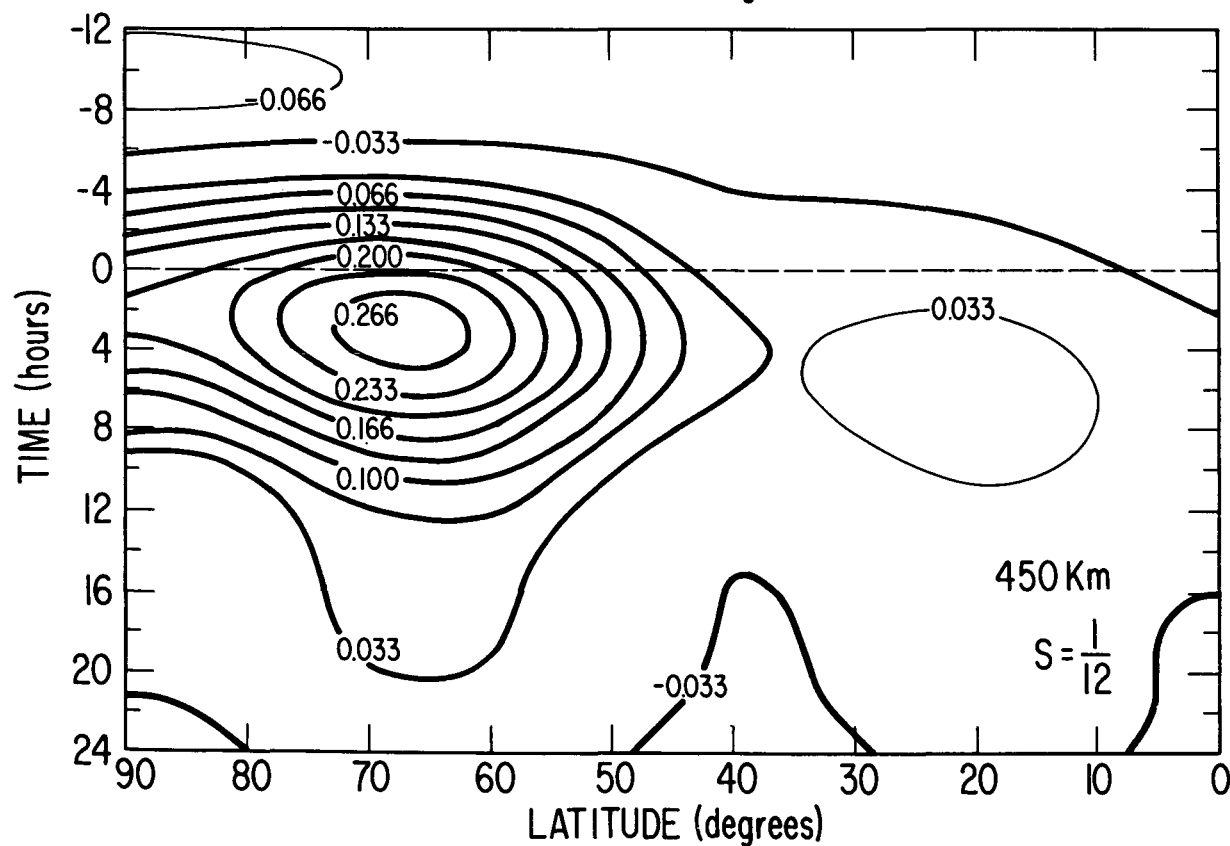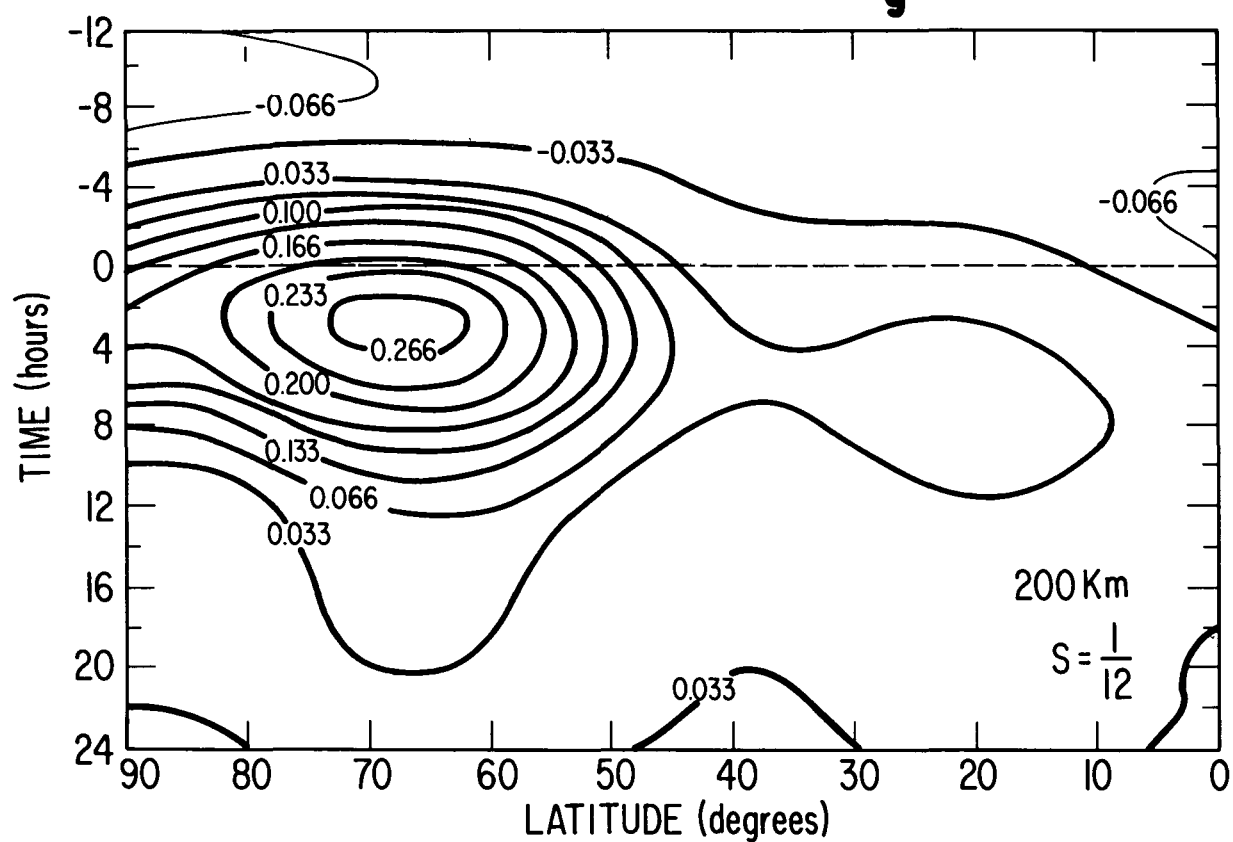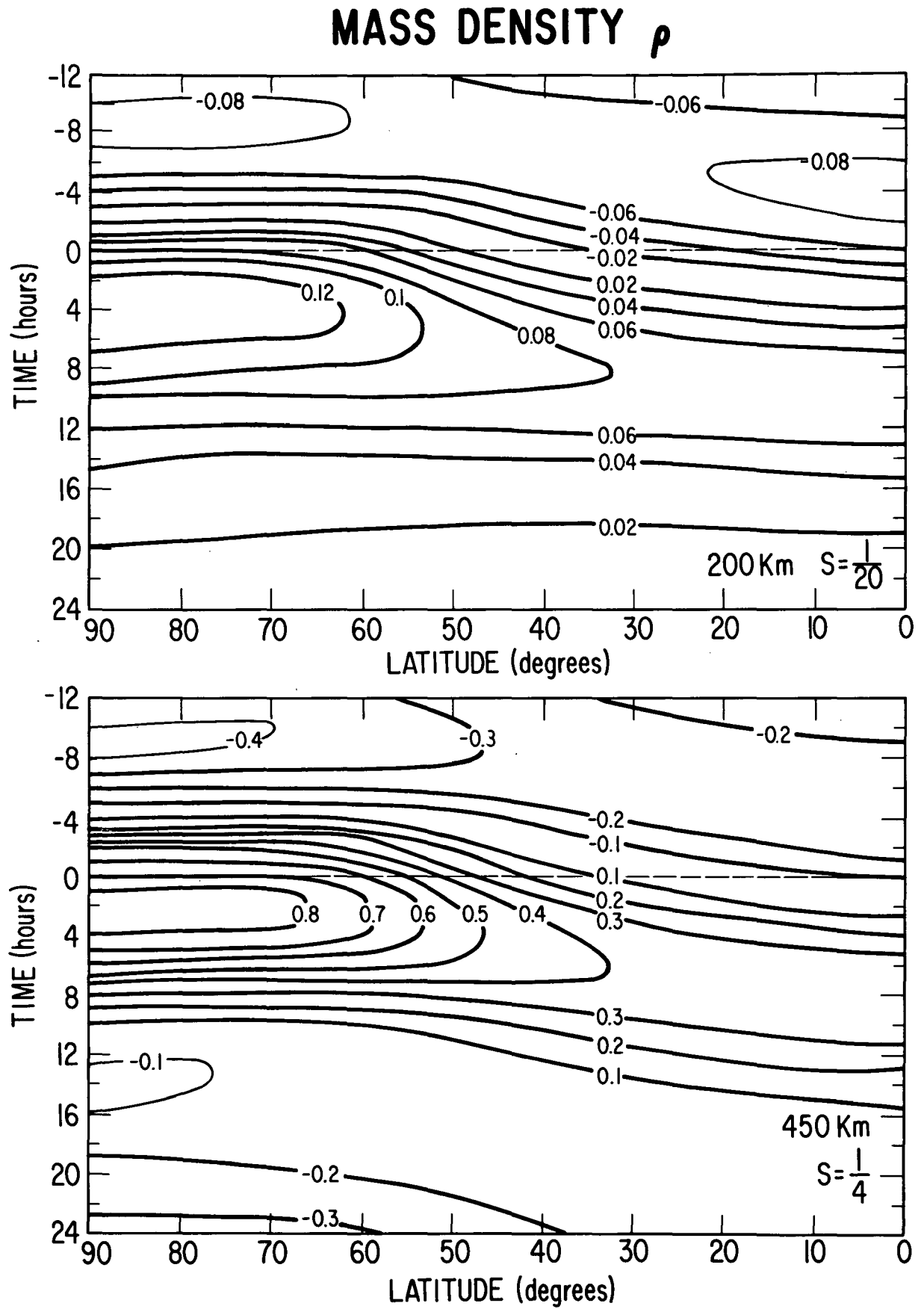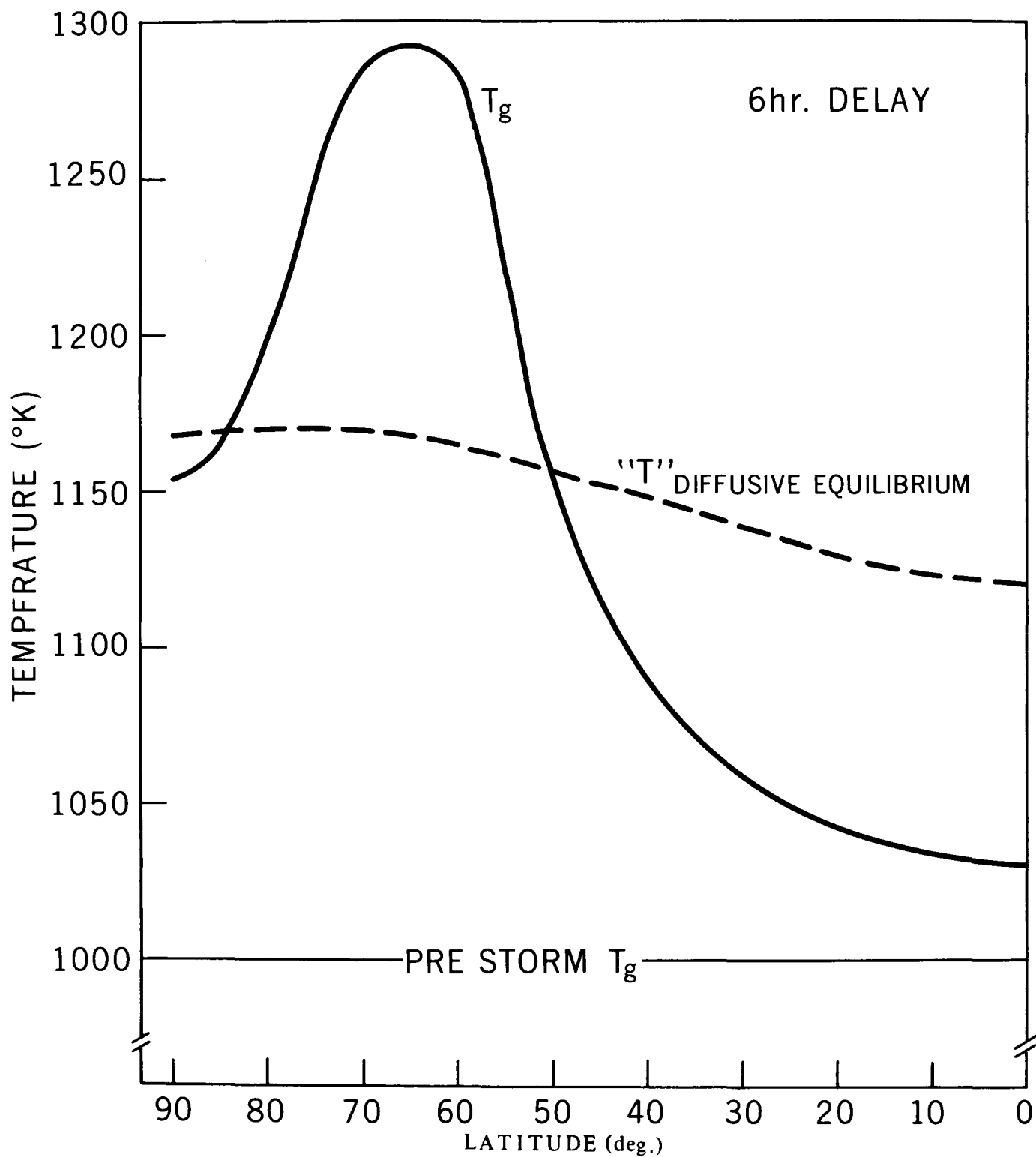
Figure 9e

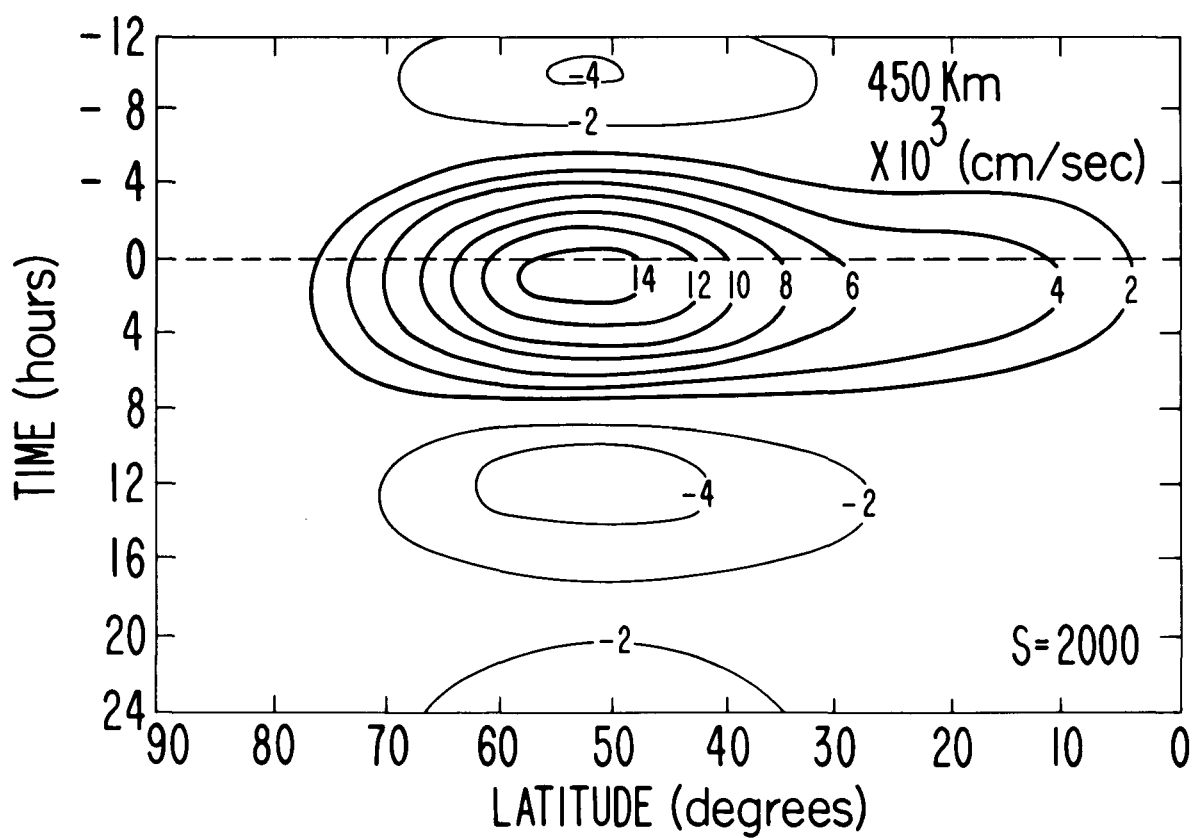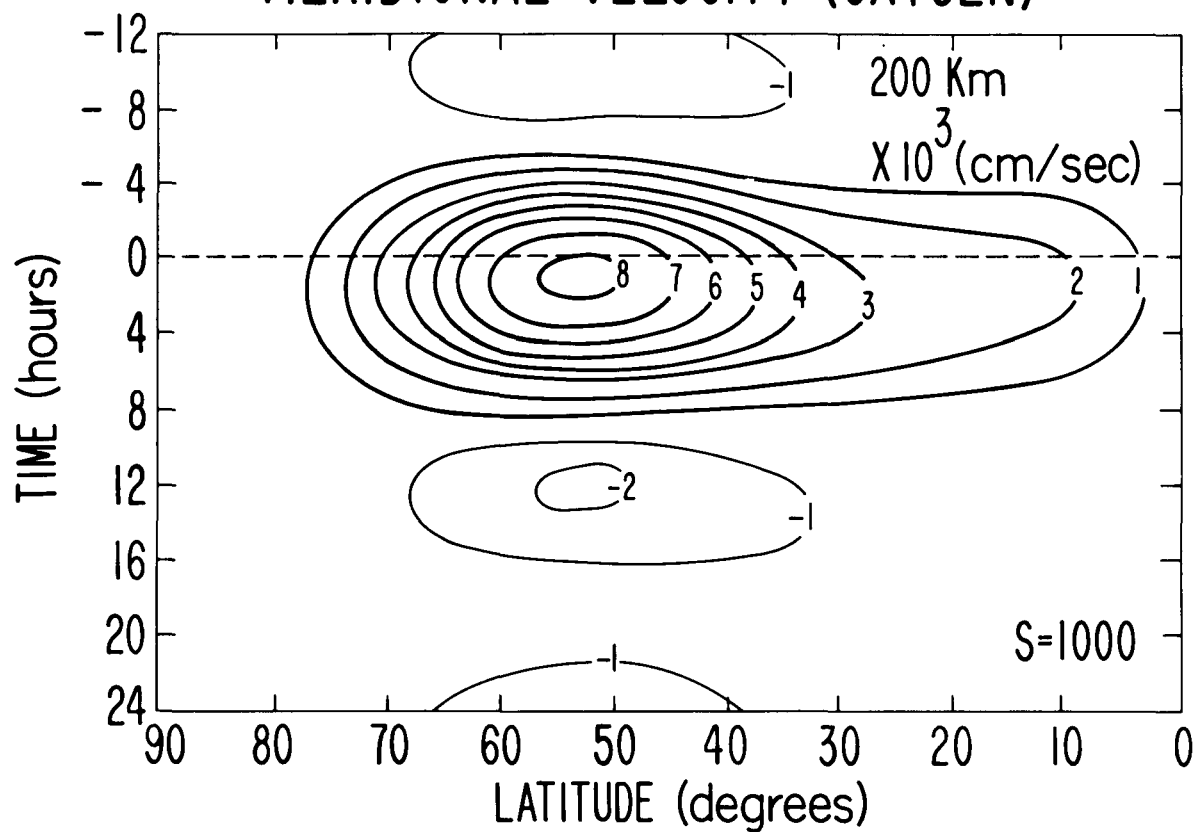Figure 10.

O/N₂ RATIO AT 200 Km
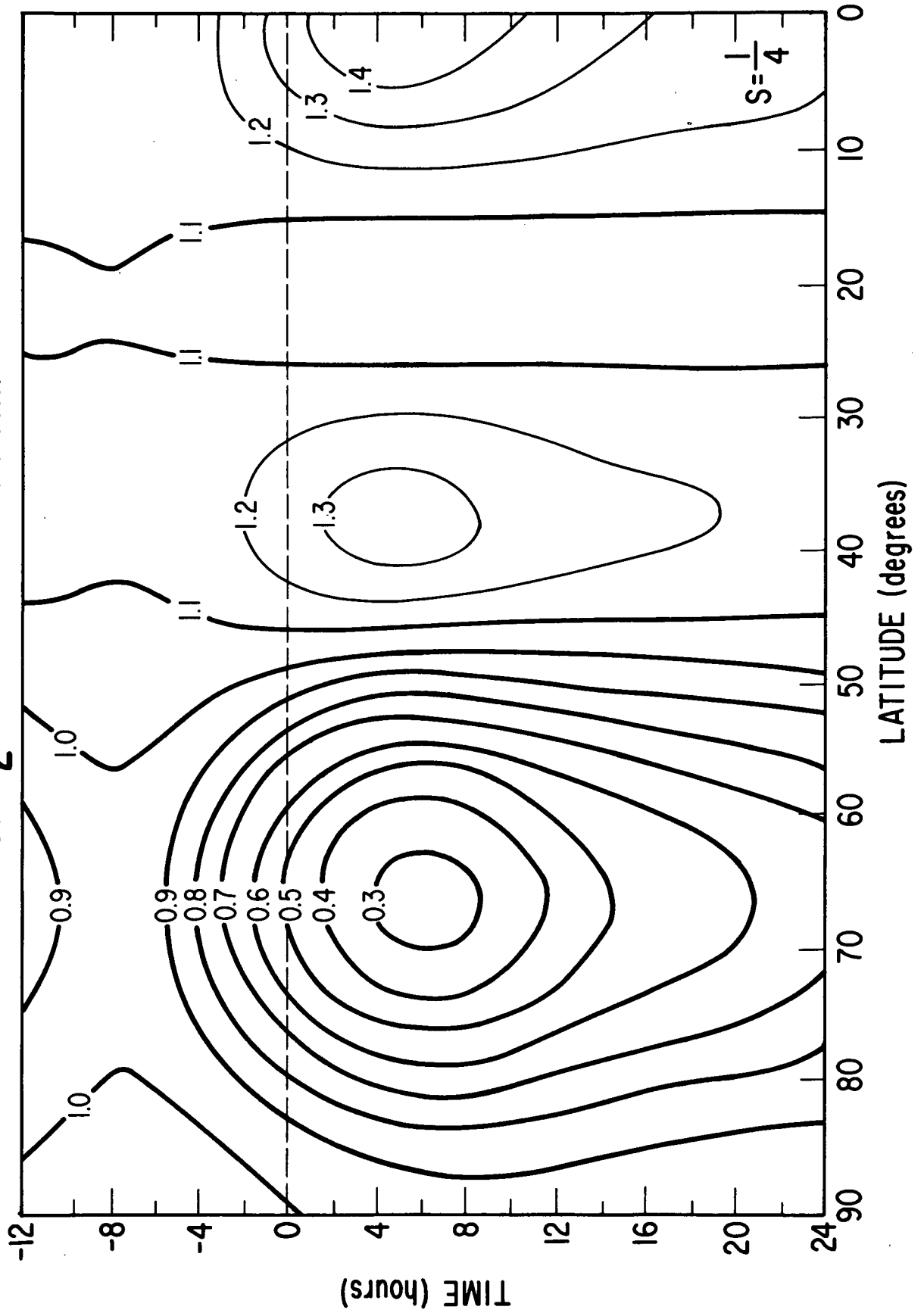
MERIDIONAL VELOCITY (OXYGEN)
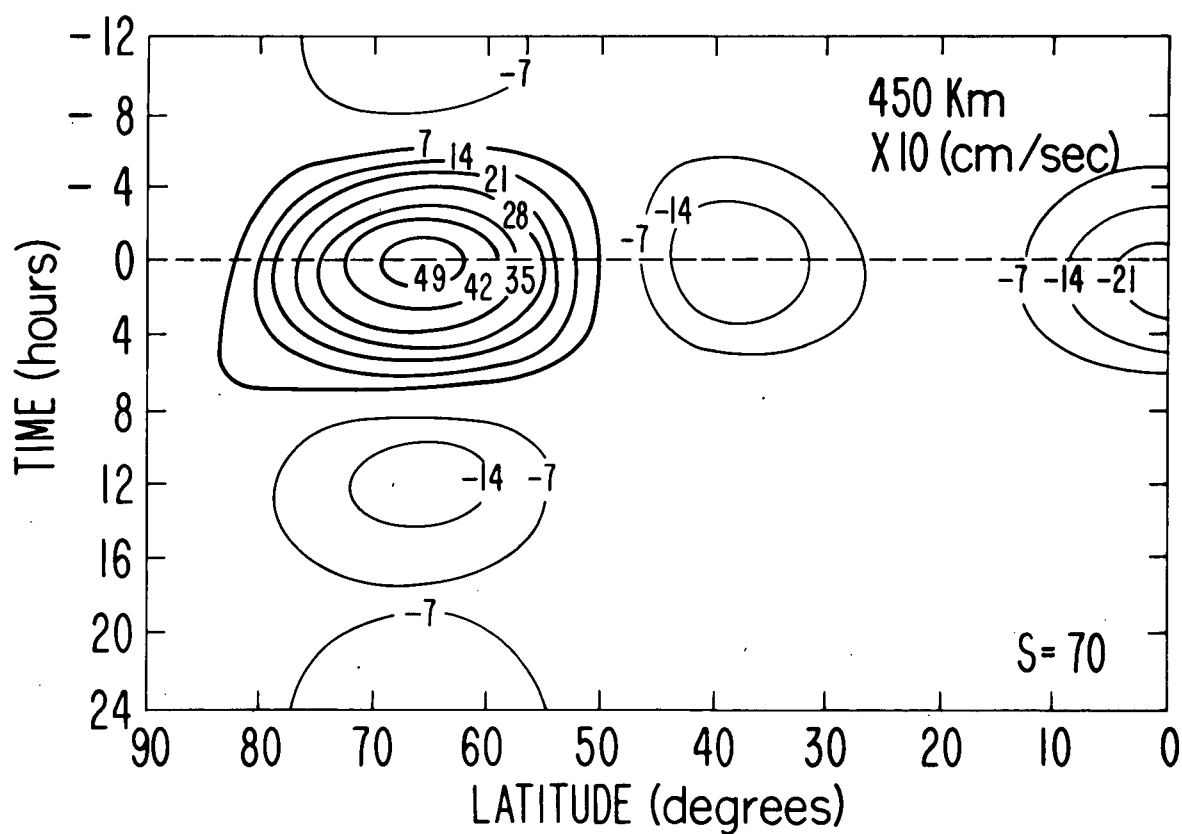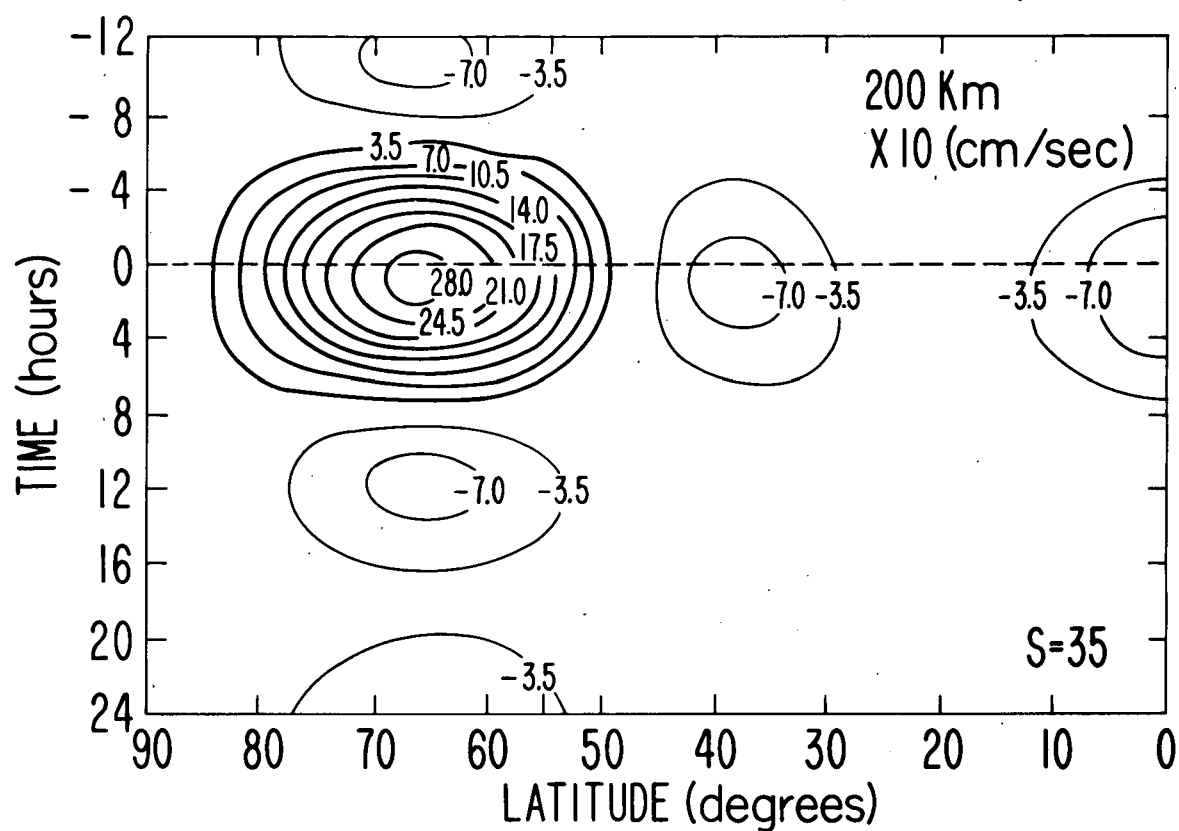

Figure 12.

VERTICAL VELOCITY (OXYGEN)

Figure 13